

# NANOPTERA IN A PERIOD-2 TODA CHAIN

CHRISTOPHER LUSTRI<sup>†</sup> AND MASON A. PORTER<sup>‡</sup>

## Abstract.

We study asymptotic solutions to singularly-perturbed period-2 discrete particle systems governed by nearest-neighbor interactions. An illustrative example, we investigate a period-2 Toda lattice and use exponential asymptotics to study exponentially small wave trains—including constant-amplitude waves called “nanoptera”—that arise near the fronts of solitary waves. Such dynamics are invisible to ordinary asymptotic-series methods. We support our asymptotic analysis with numerical computations, and finally we consider a general class of lattice equations with nearest-neighbor interactions and determine a criterion for the existence of asymptotic solutions that contain nanoptera.

## Key words.

solitary waves, exponential asymptotics, nanoptera, Toda lattice

## AMS subject classifications.

34E15, 35Q51, 34C15, 37K10

**1. Introduction.** We examine the dynamics of a spatially-localized wave propagating along a chain of particles, where the dynamics of each particle is governed by an interaction potential between it and its nearest neighbors. Systems of this form have been studied with a variety of different interaction potentials—including in celebrated models such as the Toda lattice [67] and the Fermi–Pasta–Ulam problem [27, 57] and in experimental systems such as granular crystals (via Hertzian interactions) [50, 56, 62] and their generalizations (see, e.g., [10, 29, 39]), chains of magnets [49], and more.

Classical examples of lattice systems such as the Toda lattice have been studied extensively both because of their intrinsic theoretical interest and because they play important roles in several applications, including nonlinear optical propagation [5] and electrical propagation through transmission lines [33, 42]. The Toda-lattice equations also provide a paradigmatic example of a discrete integrable system. Consequently, properties associated with the integrability of the Toda-lattice equations have been the subject of numerous studies. In particular, the integrability of the Toda lattice allows it to support soliton solutions [67].

Numerous studies have considered “uniform” one-dimensional (1D) lattices, which are chains in which each particle in the lattice is identical. However, particles need not be identical, and examinations of such “heterogeneous” lattices [43], with either periodic [35, 36, 55] or random [28, 46] distributions of different particles, reveal a wealth of fascinating dynamics that do not arise in uniform lattices. Such dynamics include new families of solitary waves that have been observed in diatomic granular chains and which can exist only for discrete values of the ratio

---

<sup>†</sup>Department of Mathematics, University of Sydney, Sydney, Australia (christopher.lustri@sydney.edu.au).

<sup>‡</sup>Oxford Centre for Industrial and Applied Mathematics, Mathematical Institute, Oxford OX2 6GG, UK; CABDyN Complexity Centre, University of Oxford, Oxford OX1 1HP, UK; and Department of Mathematics, University of California, Los Angeles, Los Angeles, California 90095, USA (mason@math.ucla.edu).

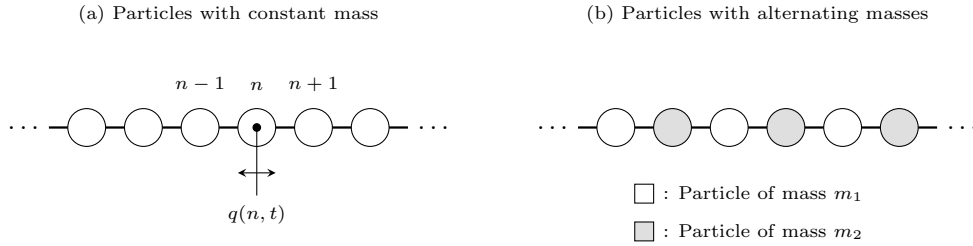


Fig. 1.1: (a) A uniform particle chain. The quantity  $q(n, t)$  represents the horizontal displacement of the particle in position  $n$  from its equilibrium position at time  $t$ . (b) A period-2 particle chain that consists of alternating particles with different masses.

between the masses of the two particles in a dimer unit [35].

In the present study, we apply asymptotic techniques to consider the behavior of propagating waves in diatomic (i.e., “period-2”) lattices, in which two different types of structures alternate with each other. Specifically, we consider bidisperse lattice systems, in which there are two different types of particles, that consist of alternations between a single heavy particle and a single light particle. See Figure 1.1 for a schematic. The primary purpose of our paper is to investigate the behavior of solitary waves in the period-2 Toda lattice in the limit in which the ratio between the heavy and light particles becomes small (i.e.,  $m_2/m_1 \rightarrow 0$ ). In particular, motivated by previous numerical and experimental studies [41, 51], we will study solutions to these period-2 Toda lattice systems that demonstrate nonlocal solitary waves (i.e., so-called “nanopterons”).

**1.1. Diatomic chains.** One of the earliest investigations of the 2-periodic Toda lattice was a numerical study of the near-integrable properties of the system by Casati & Ford [16]. This study showed that the diatomic system behaves as a near-integrable system for values of the mass ratio  $m_2/m_1 \in (0, 1)$  (where we note that the system is integrable for  $m_2/m_1 = 0$  and  $m_2/m_1 = 1$ ) if the total system energy is below some critical threshold, which depends on the mass ratio. If the total energy in the system exceeds this threshold, then the system transitions from near-integrable to chaotic behavior. However, for the purposes of the present study, we treat the system as near-integrable, as we only consider small mass ratios ( $0 < m_2/m_1 \ll 1$ ), and then the threshold energy tends to infinity as the system nears the integrable behavior associated with  $m_2/m_1 = 0$ .

The knowledge that the diatomic Toda lattice exhibits near-integrable behavior inspired many authors to search for solitary-wave solutions to these periodic systems. Early results established that these lattices do not produce the localized pulse-like solutions typically associated with the Toda Lattice [66]. Nevertheless, numerical studies such as [34, 51, 65], as well as experimental studies using electrical transmission lines [41], indicate that any solitary wave propagating through a diatomic Toda lattice leaves a trail of non-decaying oscillations in its wake. In particular, the work of Okada, *et al.* [51] suggests that the amplitude of these oscillations decays exponentially in the small mass ratio limit, so such a system is a natural setting to analyze using

exponential asymptotic methods.

The earliest analytical work on the behavior of solitary waves in a diatomic Toda lattice system was in Dash and Patanaik [20], who extended the work of Toda on the uniform lattice to identify solitary-wave behavior. Their solutions were complex-valued and hence not physical [47], but their results suggested that analytical methods can be adapted to the diatomic problem.

Several studies have examined the dynamics of solitary waves in a variety of different diatomic lattices, including systems with cubic and quartic nearest-neighbor potentials [21,54,71], Lenard–Jones potentials [17], Klein–Gordon lattice chains [40], and Fermi–Pasta–Ulam systems [59]. An important example for engineering applications is diatomic granular crystals (with alternating heavy and light particles), which have been studied both experimentally [55] and numerically and asymptotically [35,36,55]. Granular crystals have Hertzian interactions between neighboring particles, and they exhibit fascinating resonant behavior for discrete sets of mass ratios [35]. These resonances produce discrete families of solitary waves with monotonically decaying tails, even though Hertzian chains generically produce nonlocal solitary wave solutions. Similar phenomena have also been studied both numerically and analytically for a variety of “mass-in-mass” periodic particle chain configurations [37,44,70], and we will discuss such phenomena briefly in the context of the period-2 Toda lattice in Section 3.3. There have also been numerous studies of the thermal properties of period-2 Toda lattices (see, e.g., [23,32,48]), and such properties have also been studied in other diatomic particle systems, including the Fermi–Pasta–Ulam- $\beta$  lattice [72] and systems with periodic nearest-neighbor potentials [60].

Previous studies of particle chains have often utilized long-wave continuous approximations to find approximate solitary-wave solutions, such as [21,54,71]. Alternatively, previous studies such as [3] on discrete chains have expressed the exact solution in terms of integral equations; this method was used to show that localized solitary waves on monoatomic chains with power law interactions decay superexponentially in space. However, there are previous studies of diatomic systems, such as [17,35,36], in which asymptotic techniques are applied directly to the governing differential-difference equations, rather than on integral equations. In the present study, we will take this approach, and apply asymptotic series methods directly to the governing equations.

Despite the many prior studies on diatomic particle chains, there remain a wealth of avenues to further explore these systems. (In the present article, we focus on diatomic Toda chains.) The singular nature of the perturbation problem—i.e., perturbing from monoatomic a chain (which has a mass ratio of 1) to a diatomic chain, suggests that it is helpful to use exponential asymptotic techniques to asymptotically describe the behavior of waves that propagate through diatomic particle chains. This is also true for systems that are perturbations of a chain with mass ratio of 0, like the ones that we consider in our study, as such systems behave as scaled monoatomic chains (as in (3.11)). In particular, one should expect to observe trains of small waves called “nanoptera”, a form of nonlocal solitary wave that we will describe in detail in Section 1.2. The existence of these waves in the period-2 Toda lattice is suggested by numerical calculations in [51] and experimental observations in [41]. In the present study, we will derive asymptotic descriptions of these waves using exponential asymptotic methods.

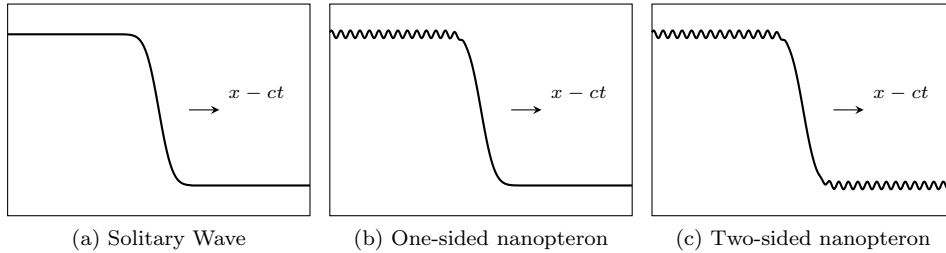


Fig. 1.2: Comparison of the profiles associated with (a) a standard solitary wave, (b) a one-sided nanopterion, and (c) a two-sided nanopterion that each propagate at speed  $c$ . The solitary wave is localized spatially, whereas the nanoptera contain non-decaying oscillatory tails on (b) one side or (c) both sides of the wave front.

The rest of our paper is organized as follows. We describe nanoptera in detail in Section 1.2, present general equations for chains with nearest-neighbor interactions in Section 1.3, present soliton solutions for the uniform one-dimensional (1D) Toda lattice in Section 1.4, and discuss the method of exponential asymptotics in Section 2. In Section 3, we use exponential asymptotics to analyze nanopterion solutions in a diatomic Toda lattice. In Section 4, we compare our analytical results to numerical computations. In Section 5, we discuss chains with more general types of nearest-neighbor interactions. We conclude in Section 6, and we present more details of our asymptotic analysis in several appendices.

**1.2. Nanoptera.** J. P. Boyd introduced the concept of a “nanopterion” in his study of the  $\phi^4$  breather [11]. Boyd used the term to describe “weakly nonlocal solitary waves”, which approximately satisfy the classical definition of a solitary wave, except that a nanopterion wave asymptotes to a small-amplitude oscillation on either one (“one-sided”) or both (“two-sided”) sides of the central solitary wave. That is, the difference between a traditional solitary wave and a nanopterion is that the latter are localized spatially only up to these small oscillations of non-decaying amplitude. Typically, these oscillations have exponentially small amplitude in the limit of some small parameter in a system, and this causes the oscillations to be invisible to standard asymptotic power-series asymptotic methods. To analyze these oscillations asymptotically, it is necessary to use exponential asymptotic techniques. In Figure 1.2, we illustrate different types of nanoptera and compare them to standard solitary waves.

Exponential asymptotic techniques, such as those developed in [7,8,18,52], can be used to capture the exponentially-small oscillations associated with nanoptera. These techniques have been used previously to find nanopterion solutions to a variety of singularly-perturbed continuous systems—including the fifth-order Korteweg–de Vries equation for gravity-capillary waves [30, 31, 68], a nonlinear Schrödinger equation [69], the  $\phi^4$  Klein–Gordon equation [61], and internal gravity waves [4]. See [12, 13] for a more comprehensive list of applications and a detailed background on the theory of weakly nonlocal solitary waves.

In the present paper, we apply exponential asymptotic methods to lattice systems to obtain asymptotic solutions containing nanoptera in period-2 Toda chains (as well as more general

diatomic particle systems). Solitary wave profiles that contain non-decaying small oscillations have been observed in several numerical and experimental studies of particle chains. In particular, small oscillations typical of nanopterion behavior have been noted in numerical [51] and experimental [41] studies of the period-2 Toda lattice, in numerics and experiments for period-2 granular chains [55], and experimentally in granular woodpile structures [38].

In this study, we will use exponential asymptotic techniques developed by [18, 52] to provide a mathematical description of nanopterion solutions in the period-2 Toda lattice. We perform all asymptotic analysis on the spatially-discrete system (i.e., without using any continuum or quasi-continuum approximations). We also determine a set of conditions that guarantee the existence of nanopterion solutions for a period-2 chain with a general interaction potential, and we show that a particular system describing a chain of beads with Hertzian nearest-neighbor interactions fails to satisfy these conditions.

**1.3. Nearest-Neighbor Interactions in a Particle Chain.** We consider chains of particles in which the dynamics of each particle is governed by nearest-neighbor interactions. We illustrate an example of such a system in Figure 1.1(a). The equations that govern the particle displacement of these chains is of the form

$$m\ddot{q}(n, t) = f(q(n-1, t) - q(n, t)) - f(q(n, t) - q(n+1, t)) , \quad (1.1)$$

where  $q(n, t)$  is the displacement from equilibrium of the particle located at position  $n$  and at time  $t$ , the mass of each particle is  $m$ , and  $\dot{\phantom{x}}$  indicates a derivative with respect to time. We also require boundary conditions at  $t = 0$  and as  $n \rightarrow \infty$ . We will make these conditions explicit for the case of diatomic lattices.

There have been many studies of systems of the form (1.1) that ask whether the equations admit solitary-wave solutions in the form of a spatially-localized wave that travels through the system without decaying or changing form. Solitary wave solutions have been found in many well-known particle chain systems, such as the Toda lattice [26, 67].

In the present paper, we study periodic heterogenous chains in which the component particles have different mass. In particular, as we illustrate with a schematic in Figure 1.1(b), we examine period-2 particle chains in which particles of different masses alternate with each other. We suppose that the mass ratio  $m_2/m_1$  is small, so that  $0 < m_2/m_1 \ll 1$ . (We thus say that particle 1 is the “heavy” particle and particle 2 is the “light” particle.) Imposing this configuration and scaling the system (1.1) yields

$$\ddot{y}(n, t) = f(z(n-1, t) - y(n, t)) - f(y(n, t) - z(n, t)) , \quad (1.2)$$

$$\epsilon\ddot{z}(n, t) = f(y(n, t) - z(n, t)) - f(z(n, t) - y(n+1, t)) , \quad (1.3)$$

where  $y(n, t)$  and  $z(n, t)$ , respectively, are the displacement of the heavy and light particles, and the mass ratio is  $m_2/m_1 = \epsilon$ . We illustrate this configuration in Figure 1.3.

To fully specify the solution to the system (1.2,1.3), we also need initial conditions for  $y(n, t)$ ,

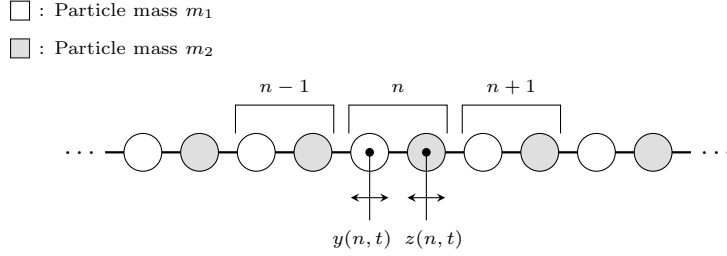


Fig. 1.3: Setup for the Toda chain with alternating particle masses. Instead of individual particle labels, we label each pair; we use  $y(n, t)$  to denote the displacement of the first particle in the pair and use  $z(n, t)$  to denote the displacement of the second particle.

$z(n, t)$ , and their first-order time derivatives. See Section 3.1 for a discussion of these initial conditions. Finally, we specify the spatial boundary conditions as  $n \rightarrow \infty$  so that they are consistent with the initial conditions in the same limit.

To find the leading-order behavior of (1.2,1.3), we set  $\epsilon = 0$  in (1.3). The resulting expression satisfies

$$z(n, t) = \frac{1}{2} [y(n, t) + y(n + 1, t)] . \quad (1.4)$$

We can therefore eliminate  $z(n, t)$  from equation (1.2) to obtain

$$\ddot{y}(n, t) = f\left(\frac{1}{2}[y(n-1, t) - y(n, t)]\right) - f\left(\frac{1}{2}[y(n, t) - y(n+1, t)]\right) , \quad (1.5)$$

which is a scaled version of the nearest-neighbor equation (1.1). Consequently, one can obtain solutions to the  $\epsilon = 0$  version of the system (1.2,1.3) by appropriately scaling solutions to the original nearest-neighbor equation. We will therefore use solitary-wave solutions to the  $\epsilon = 0$  case as the basis for an asymptotic study of the full system (1.2,1.3), in which  $\epsilon$  is a small positive parameter.

We use techniques from exponential asymptotics to show that some variants of the system (1.2,1.3) produce solutions that containing nanoptera and depend on the choice of nearest-neighbor potential. We will show that the period-2 Toda lattice permits nanopteron solutions, and we will determine their functional form. Finally, we will consider the general case (1.2,1.3) and determine a sufficient condition on the function  $f$  for the presence of nanopteron solutions.

**1.4. Solitons in the Toda-Lattice Equation.** For convenience, we first consider the nearest-neighbor dynamics to be governed by the Toda-lattice equation

$$\ddot{q}(n, t) = e^{-[q(n, t) - q(n-1, t)]} - e^{-[q(n+1, t) - q(n, t)]} . \quad (1.6)$$

It is well-known that equation (1.6) possesses closed-form soliton solutions [67], which will be

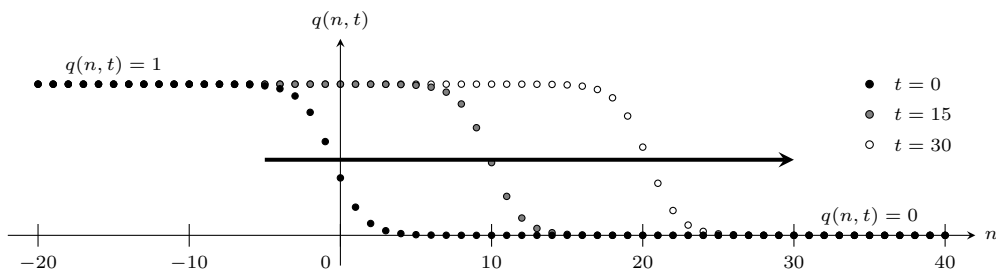


Fig. 1.4: A single soliton, of the form (1.7), traveling through a Toda chain. The parameter values are  $\gamma = 1$ ,  $\kappa = 1/2$ ,  $\sigma = 1$ , and  $q_+ = 0$ . The speed of the moving front is  $\sigma \sinh(\kappa)/\kappa \approx 1.0422$ .

helpful for our analysis. The simplest of these soliton solutions is the 1-soliton solution

$$q(n, t) = q_+ + \log \left( \frac{1 + \alpha \exp(-2\kappa n + 2\sigma \sinh(\kappa)t)}{1 + \alpha \exp(-2\kappa(n-1) + 2\sigma \sinh(\kappa)t)} \right), \quad (1.7)$$

with  $\kappa, \alpha > 0$  and  $\sigma \in \{\pm 1\}$ . The solution (1.7) describes a bump of width proportional to  $1/\kappa$  that travels through a medium with speed  $\pm \sinh(\kappa)$ . In Figure 1.4, we show an example of this solution.

More general  $N$ -soliton solutions to the Toda-lattice equation also exist, and they are given in closed form by

$$q(n, t) = q_+ + \log \left( \frac{\det(I_N + C_N(n, t))}{\det(I_N + C_N(n-1, t))} \right), \quad (1.8)$$

where  $I_N$  denotes the  $N \times N$  identity matrix, and

$$C_N(n, t) = \frac{\sqrt{\alpha_j \alpha_k} \exp\{-(\kappa_j + \kappa_k)n - (\sigma_j \sinh(\kappa_j) + \sigma_k \sinh(\kappa_k))t\}}{1 - e^{-(\kappa_j + \kappa_k)}}, \quad j, k \in \{1, \dots, N\}, \quad (1.9)$$

where  $\kappa_j, \alpha_j > 0$  and  $\sigma_j \in \{\pm 1\}$ . In the present paper, we restrict our attention to the 1-soliton solution, but we discuss extensions to the  $N$ -soliton solution in Section 6.

For a singularly-perturbed system of the form (1.2,1.3) with a Toda interaction potential between particles, we will use the soliton solutions that we introduced in this section to construct nanopteron solutions.

**2. Exponential Asymptotics and Stokes Curves.** We will determine the asymptotic behavior of exponentially-small, non-decaying waves that appear in the wake of the solitary-wave front. However, determining the behavior of terms that are exponentially small compared to the leading-order solution in the  $\epsilon \rightarrow 0$  asymptotic limit is impossible using classical asymptotic series expansions, because the exponentially-small contribution is necessarily smaller than any power of the small parameter  $\epsilon$ . Therefore, we must apply specialized techniques, known as *exponential asymptotics*, to determine behavior on this scale [12, 13].

As we uncover this exponentially-small behavior, we will see that the analytic continuation of the solution contains curves known as ‘‘Stokes curves’’ [64]. These curves are related to the

behavior of exponentially-small components of the solutions. As Stokes curves are crossed, the exponentially-small contribution experiences a smooth, rapid change in value in the neighborhood of the curve. In many problems, including the present investigation, the exponentially-small contribution to the solution appears only on one side of the Stokes curve.

The central idea of exponential asymptotic methods is that one can truncate a divergent asymptotic series to provide a useful approximation to some exact solution. Additionally, one can choose the truncation point to minimize the error between the approximation and the exact solution; this is known as *optimal truncation*. Importantly, when a divergent series is truncated optimally, the associated approximation error is generally exponentially small in the asymptotic limit [13]. One can then rescale the problem to directly determine this approximation error, allowing the exponentially-small component of the solution to be determined in the absence of the asymptotic series itself. This idea was introduced by Berry [7, 8], and it was employed in [6, 9] to determine the position of Stokes curves in special functions such as the Airy function and to examine the smooth nature of the associated switching behavior.

In the present paper, we will apply an exponential asymptotic method developed by Olde Daalhuis et al. [52] for linear differential equations and extended by Chapman et al. [18] to nonlinear ordinary differential equations. We provide a brief outline of the process. See the above papers for a more detailed explanation of the methodology.

The first step in exponential asymptotic analysis is to express the solution as an asymptotic power series. In many singularly-perturbed problems, including those that we consider in the present study, the asymptotic series solution takes the form of a divergent series. For a more detailed discussion of asymptotic series divergence, see [14, 24]. One can minimize the approximation error by truncating the series optimally. However, this requires a general form for the asymptotic series coefficients, and it is often algebraically intractable to obtain such a general form. In practice, however, one does not require the exact form of the series coefficients. Instead, one needs only the so-called *late-order terms*, which are asymptotic expressions for the  $r$ th series coefficient in the  $r \rightarrow \infty$  limit

In singular perturbation problems, Darboux [19] noted that one can obtain successive terms in an asymptotic series expansion by repeated differentiation of an earlier term in the series. Specifically, assume that we have some function  $\phi(z)$  on  $z \in \mathbb{C}$  that can be expanded within a circle as a Taylor–Maclaurin series  $\sum_0^\infty \psi_r z^r$ . If we let  $z_s$  represent the location of the nearest non-essential singularity on or outside the circle of convergence, we can write

$$\phi(z) = (z_s - z)^{-p_s} \phi_s(z), \quad (2.1)$$

where  $p_s$  is either fractional (for branch points) or a positive integer (for poles), and  $\phi_s(z)$  can be expanded as a Taylor series about  $z_s$ . Darboux [19] showed that the behavior of  $\psi_r$  in the limit that  $r \rightarrow \infty$  follows a predictable form, satisfying

$$\psi_r \sim \frac{\phi_s(z_s) \Gamma(r + p_s)}{\Gamma(r + 1) (p_s - 1) z_s^{r+p_s}} \quad \text{as} \quad r \rightarrow \infty, \quad (2.2)$$

where  $\Gamma$  is the gamma function [1, 2, 53]. Dingle [24] gave a detailed derivation of the expression (2.2). Dingle also considered the case in which there are multiple equidistant singularities, and demonstrated by example that their contributions can simply be summed to correctly approximate the late-order terms of the power-series expansion. This is also true of the behavior that we consider in the present study.

From (2.2), we see that the late-order terms of the resulting asymptotic series diverge as the ratio between a factorial and the increasing power of a function  $\chi$ . Noting the factorial-over-power form in (2.2), Chapman et al. [18] proposed writing an ansatz for the late-order terms that is capable of describing this form of late-order term behavior. One writes

$$\psi_r \sim \frac{\Psi\Gamma(r + \gamma)}{\chi^{r+\gamma}} \quad \text{as } r \rightarrow \infty, \quad (2.3)$$

where  $\Psi$ ,  $k$ , and  $\chi$  are functions that do not depend on  $r$ , but are free to vary with independent variables in the problem, such as, say,  $z$ . In particular, the “singulant”  $\chi$  equals 0 at values of  $z$  where the leading-order behavior  $\psi_0$  is singular, denoted by  $z = z_s$ . This ensures that the late-order ansatz for  $\psi_r$  also has a singularity at  $z = z_s$  and that the singularity increases in strength as  $r$  increases. One can then use the ansatz (2.3) to optimally truncate an asymptotic expansion. The method developed in Olde Daalhuis et al. [52] involves substituting the resulting truncated series expression into the original problem to obtain an equation for the exponentially-small remainder term.

The exponentially-small contribution to the asymptotic solution that is calculated using this method generally takes the form  $\mathcal{S}Ae^{-\chi/\epsilon}$ , where the “Stokes multiplier”  $\mathcal{S}$  rapidly varies from 0 to a nonzero value as one crosses a Stokes curves. The variation is smooth, and it occurs in a neighborhood of width  $\mathcal{O}(\sqrt{\epsilon})$  that surrounds the Stokes curve. This behavior is known as *Stokes switching*, and it occurs along curves at which the switching exponential is maximally subdominant and hence where the singulant  $\chi$  is real and positive [9].

Examining when a Stokes multiplier becomes nonzero provides a simple criterion to determine where the exponentially-small contribution to a solution “switches on” and cannot be ignored. One finds the positions of Stokes curves by determining the curves along which the singulant is real and positive. Consequently, exponential asymptotic analysis makes it possible to (1) determine the form of exponentially-small contributions to a solution and (2) determine the regions of a solution domain in which the contribution is present. In the present study, these contributions take the form of an exponentially-small wave train that follows the leading-order solitary wave. In other words, they give us nanoptera.

See the review article [13] or monograph [12] for more details on exponential asymptotics and their application to nonlocal solitary waves. References [7, 8, 14] are examples of previous studies of exponential asymptotics. Finally, see [18, 52] for more details on the particular methodology that we apply in the present paper.

### 3. Period-2 Toda Lattice.

**3.1. Formulation and Series Solution.** We consider the period-2 form of the Toda-lattice equation associated with the system (1.2,1.3). It is typically written as

$$\ddot{y}(n, t) = e^{-[y(n, t) - z(n-1, t)]} - e^{-[z(n, t) - y(n, t)]}, \quad (3.1)$$

$$\epsilon \ddot{z}(n, t) = e^{-[z(n, t) - y(n, t)]} - e^{-[y(n+1, t) - z(n, t)]}, \quad (3.2)$$

where  $0 < \epsilon \ll 1$ , and we recall that  $\epsilon$  is proportional to the ratio between the masses of the light and heavy particles in a chain. In general, the system (3.1,(3.2)) requires two initial conditions each at  $t = 0$  for  $y(n, t)$  and  $z(n, t)$ . However, to construct a nonlocal solitary-wave solution, we instead specify a particular leading-order solution of the system (associated with  $\epsilon = 0$ ) at the appropriate stage of the analysis. We denote these leading-order expressions by  $y_0(n, t)$  and  $z_0(n, t)$ . In practice, this is equivalent to posing the problem with initial conditions

$$y(n, 0) = y_0(n, 0), \quad \dot{y}(n, 0) = \dot{y}_0(n, 0), \quad z(n, 0) = z_0(n, 0), \quad \dot{z}(n, 0) = \dot{z}_0(n, 0). \quad (3.3)$$

Finally, we specify that the particles ahead of the solitary-wave front are undisturbed, which entails that

$$y(n, t) \rightarrow y_0(n, t) \quad \text{as } n \rightarrow \infty, \quad z(n, t) \rightarrow z_0(n, t) \quad \text{as } n \rightarrow \infty. \quad (3.4)$$

This ensures that nonlocal oscillations remain in the wake of the solitary-wave front and consequently that any ensuing nanopterion solutions are one-sided.

We are interested in traveling solitary-wave solutions, so we define the variable

$$\xi = n - \frac{\sigma \sinh(\kappa)t}{\kappa\sqrt{2}}, \quad (3.5)$$

which gives a frame that moves with the solitary wave. This frame is consistent with the 1-soliton solution (1.7). We thereby represent the Toda system by the coupled delay-differential equations (DDEs)

$$\lambda y''(\xi) = e^{-[y(\xi) - z(\xi-1)]} - e^{-[z(\xi) - y(\xi)]}, \quad (3.6)$$

$$\epsilon \lambda z''(\xi) = e^{-[z(\xi) - y(\xi)]} - e^{-[y(\xi+1) - z(\xi)]}, \quad (3.7)$$

where  $\lambda = \sinh^2(\kappa)/2\kappa$  and  $'$  denotes differentiation with respect to  $\xi$ . Note that our subsequent analysis does not require a moving reference frame. It is a convenient frame when considering the 1-soliton solution, but it does not provide any advantage when considering problems with multiple solitary waves. To treat such situations, we note that our analysis below can be used in a stationary reference frame with only minor modifications to the subsequent analysis. In such a scenario, we could not use the continuous variable  $\xi$  but would instead treat  $n$  as a parameter and apply our analysis directly to the system (3.1,3.2), with  $t$  as a continuous independent variable. See Section 5.

Previous studies, such as [3], examined systems of the form (3.1,3.1) by writing the solution

in terms of integral equations. In contrast, we apply asymptotic-series methods directly to the differential-difference system in (3.6,3.7). By using these methods, we will be able to directly study exponentially small oscillations in the solutions.

We expand the dependent variables as a series in  $\epsilon$  and write

$$y(\xi) \sim \sum_{j=0}^{\infty} \epsilon^j y_j(\xi), \quad z(\xi) \sim \sum_{j=0}^{\infty} \epsilon^j z_j(\xi). \quad (3.8)$$

Inserting equation (3.8) into equations (3.1,3.2) yields

$$\lambda \sum_{j=0}^{\infty} \epsilon^j y_j''(\xi) = \exp\left(-\sum_{j=0}^{\infty} \epsilon^j [y_j(\xi) - z_j(\xi - 1)]\right) - \exp\left(-\sum_{j=0}^{\infty} \epsilon^j [z_j(\xi) - y_j(\xi)]\right), \quad (3.9)$$

$$\lambda \sum_{j=0}^{\infty} \epsilon^{j+1} z_j''(\xi) = \exp\left(-\sum_{j=0}^{\infty} \epsilon^j [z_j(\xi) - y_j(\xi)]\right) - \exp\left(-\sum_{j=0}^{\infty} \epsilon^j [y_j(\xi + 1) - z_j(\xi)]\right). \quad (3.10)$$

Using a standard asymptotic power series approach to (3.9,3.10) entails expanding about  $\epsilon = 0$  and matching to leading order in  $\epsilon$ . With the canonical linear-in- $\epsilon$  expansion, we obtain

$$\lambda y_0''(\xi) = e^{-\frac{1}{2}[y_0(\xi) - y_0(\xi - 1)]} - e^{-\frac{1}{2}[y_0(\xi + 1) - y_0(\xi)]}, \quad z_0(\xi) = \frac{1}{2}[y_0(\xi + 1) + y_0(\xi)]. \quad (3.11)$$

Recall the observation from Section 1.4 that the  $\epsilon = 0$  case of a period-2 particle system of the form (1.2,1.3) is simply a scaled version of the equivalent constant-mass system. Consequently, one can obtain the solutions for  $y_0(\xi)$  in equation (3.11) by appropriately scaling a solution of the one-variable Toda-lattice equation (1.6). In this case, we begin with a 1-soliton solution (1.7) in terms of the original variables. By scaling this solution and noting that  $\xi$  takes the form in equation (3.5), we find that the leading-order behavior of the 1-soliton solution for the system (3.1,3.2) is

$$y_0(\xi) = y_+ + \log\left(\frac{1 + \alpha \exp(-2\kappa\xi)}{1 + \alpha \exp(-2\kappa(\xi + 1))}\right), \quad (3.12)$$

$$z_0(\xi) = y_+ + \frac{1}{2} \log\left(\frac{1 + \alpha \exp(-2\kappa\xi)}{1 + \alpha \exp(-2\kappa(\xi + 2))}\right), \quad (3.13)$$

where  $y_+$ ,  $\kappa$ , and  $\alpha$  are parameters. In Figure 3.1, we show  $z(\xi)$  for an example of a solitary wave with this leading-order behavior. Note that Figure 3.1 depicts the propagating solitary wave after all transient radiative effects have disappeared. This solution has parameter values  $y_+ = -1$ ,  $\kappa = 1$ , and  $\alpha = 1$ ; and it is associated with a leading-order solution that takes the value  $z = -2$  ahead of the solitary wave and  $z = 2$  behind the solitary-wave front.

One can compute subsequent terms in the series using equations (3.9,3.10) and the recursion relation

$$\lambda y_j''(\xi) = -[y_j(\xi) - z_j(\xi - 1)]e^{-[y_0(\xi) - z_0(\xi - 1)]} + [z_j(\xi) - y_j(\xi)]e^{-[z_0(\xi) - y_0(\xi)]} + \dots, \quad (3.14)$$

$$\lambda z_{j-1}''(\xi) = -[z_j(\xi) - y_j(\xi)]e^{-[z_0(\xi) - y_0(\xi)]} + [y_j(\xi + 1) - z_j(\xi)]e^{-[y_0(\xi + 1) - z_0(\xi)]} + \dots, \quad (3.15)$$

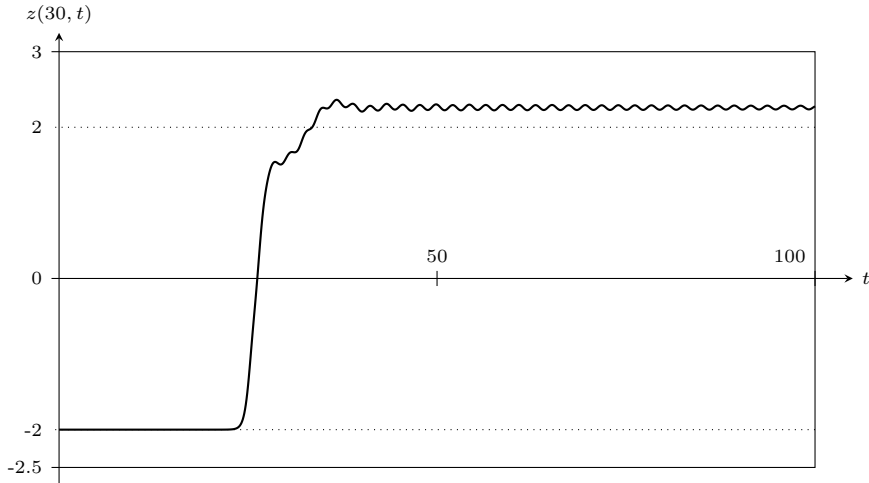


Fig. 3.1: A nanoperturbation propagating through an individual particle ( $n = 30$ ) in a singularly-perturbed period-2 Toda chain with mass ratio  $\epsilon = 0.2$ , where the particle is one of the lighter particles in the chain. The leading-order behavior is a localized solitary wave that varies from  $z = -2$  (where  $z$  represents the position of the particle) in front of the wave to  $z = 2$  behind the wave. In addition to the wave train, which is exponentially small in  $\epsilon$ , the asymptotic solution behind the wave train has an  $\mathcal{O}(\epsilon)$  offset from the leading-order solitary wave. We obtained this solution from the computations that produced Figure 4.1.

where the omitted terms are subdominant as  $j$  becomes large. Unfortunately, it is difficult to solve equations (3.14,3.15) analytically (even just for the first correction term) in terms of a closed-form expression. However, the wave train has exponentially-small amplitude and it hence lies beyond the reach of this asymptotic power-series approach. Consequently, it will not be helpful to obtain correction terms to the asymptotic power series. Instead, we will apply exponential asymptotic methods to determine the behavior of these trailing waves.

We also note that the general problem in equations (1.2,1.3) need not possess a convenient closed-form soliton solution to the associated  $\epsilon = 0$  system. Thankfully, as we will illustrate in Section 5, this does not necessarily prevent one from drawing useful conclusions about the asymptotic behavior of associated solutions.

**3.2. Late-Order Terms.** As we discussed in Section 2, we need to ascertain the behavior of the terms in the series (3.8) in the limit that  $j \rightarrow \infty$  to determine the exponentially-small component of the solution. Unfortunately, it is difficult to exactly compute even the first correction term of the series. Instead, we follow the process described by Chapman et al. [18] and apply a factorial-over-power ansatz similar to equation (2.3) to approximate these late-order terms in the  $j \rightarrow \infty$  limit. Hence, we assume that the late-order terms are given by a sum of expressions with the form

$$y_r(\xi) \sim \frac{Y(\xi)\Gamma(2r + \gamma_1)}{\chi(\xi)^{2r + \gamma_1}}, \quad z_j(\xi) \sim \frac{Z(\xi)\Gamma(2r + \gamma_2)}{\chi(\xi)^{2r + \gamma_2}}, \quad (3.16)$$

where  $\gamma_1$  and  $\gamma_2$  are constants, and  $Y$ ,  $Z$ , and  $\chi$  are functions of  $\xi$  but not functions of  $r$ . We also analytically continue  $\xi$  so that  $\xi \in \mathbb{C}$ . Recall that the singulant  $\chi$  is particularly important, as it permits singularities in the leading-order behavior to propagate into late-order terms. It is equal to 0 at points  $\xi = \xi_s$  in the complex plane at which the leading-order behavior is singular. Obtaining each successive term in the sequence requires second-order differentiation, so we expect the argument of the gamma function, and hence the power of the singularity, to increase by two in each successive term. This gives the form in the ansatz (3.16).

As we noted above, the late-order terms are given by the sum of expressions of the form (3.16). In this case, each expression is associated with a different singularity in the analytic continuation of  $z_0$ . We denote the locations of these singularities by  $\xi = \xi_r$  (where  $r \in \{1, \dots, 4\}$ ). They occur at

$$\xi_1 = \frac{1}{2\kappa}(\log \alpha + \pi i), \quad \xi_2 = \frac{1}{2\kappa}(\log \alpha - \pi i), \quad (3.17)$$

$$\xi_3 = \frac{1}{2\kappa}(\log \alpha + \pi i) - 2, \quad \xi_4 = \frac{1}{2\kappa}(\log \alpha - \pi i) - 2. \quad (3.18)$$

The analytic continuation of  $z_0$  contains other singularities; however, late-order term asymptotic behavior at any point is exponentially dominated by the nearest singularities to that point [24]. Consequently, we can neglect singularities that are further away from the real axis in this analysis.

The process of determining the components of (3.16) is technical, and we show it in Appendix A. From this analysis, we find that the terms in the ansatz (3.16) are given by

$$\lambda [\chi'_s(\xi)]^2 = -2e^{-\frac{1}{2}[y_0(\xi+1) - y_0(\xi)]}, \quad \chi_s(\xi) = 0 \quad \text{at} \quad \xi = \xi_s, \quad (3.19)$$

and  $Z_s(\xi) = \Lambda_s / \sqrt{\chi'_s(\xi)}$ , where  $\Lambda_s$  is a constant, which we compute in Appendix B.2 to be

$$\Lambda_{1,2} \approx -0.3500i \left[ \frac{2\sqrt{2\kappa}}{\lambda} \sqrt{\frac{\exp 2\kappa + 1}{\exp 2\kappa - 1}} \right], \quad \Lambda_{3,4} \approx 0.3500i \left[ \frac{2\sqrt{2\kappa}}{\lambda} \sqrt{\frac{\exp 2\kappa + 1}{\exp 2\kappa - 1}} \right]. \quad (3.20)$$

We also show in Appendix B.1 that  $\gamma_2 = -\frac{1}{10}$ . Hence, as  $j \rightarrow \infty$ , one can express the terms in the series expression (3.8) as

$$z_r(\xi) \sim \sum_{s=1}^4 \frac{\Lambda_s \Gamma(2r - \frac{1}{10})}{\sqrt{\chi'_s(\xi)} [\chi_s(\xi)]^{2r-1/10}}. \quad (3.21)$$

**3.3. Exponential Asymptotics.** The key idea of exponential asymptotics is that one can truncate an asymptotic series optimally at some term number  $N_{\text{opt}}$  such that the remainder is exponentially small. The solution can thus be expressed as

$$y(\xi) \sim \sum_{r=0}^{N_{\text{opt}}} \epsilon^r y_r(\xi) + y_{\text{exp}}(\xi), \quad z(\xi) \sim \sum_{r=0}^{N_{\text{opt}}} \epsilon^r z_r(\xi) + z_{\text{exp}}(\xi), \quad (3.22)$$

where  $y_{\text{exp}}$  and  $z_{\text{exp}}$  are exponentially small as  $\epsilon \rightarrow 0$ .

Recall from Section 2 that one can determine the exponentially-small contribution to the asymptotic solution from the form of the late-order terms, and that this contribution switches rapidly across Stokes curves. In Appendix 3.3, we apply exponential asymptotic methods directly to determine the form of the late-order terms and the associated Stokes-curve locations. In equation (C.3), we find that the optimal truncation point has the form  $N_{\text{opt}} \sim |\chi_r|/2\sqrt{\epsilon}$  as  $\epsilon \rightarrow 0$  and that the behavior after switching across Stokes curves is a sum of terms that have the form  $z_{\text{exp}} \sim \mathcal{S}_r Z_r \exp(-\chi_r/\sqrt{\epsilon})$  as  $\epsilon \rightarrow 0$ .

Recall that Stokes curves are curves in the complex plane that satisfy  $\text{Im}(\chi) = 0$  and  $\text{Re}(\chi) > 0$ . We thereby see that  $z_{\text{exp}}$  is exponentially small as  $\epsilon \rightarrow 0$ . Although it is not easy to analytically solve the singulant equation (3.19) analytically, one can obtain the solution using numerical integration. The singulant equation has two solutions, but we can discard one of them immediately, as its real part is negative everywhere on the real axis and it therefore never satisfies the Stokes-curve condition on  $\text{Re}(\chi)$ .

In Figure 3.2, we show the imaginary parts of  $\chi_1$  and  $\chi_3$  with the parameter values  $\alpha = 1$ ,  $\sigma = 1$ , and  $\kappa = 1$ . We find that  $\text{Re}(\chi_{1,3}) \approx 2.44$ , so Stokes switching takes place when  $\text{Im}(\chi_{1,3}) = 0$ . We assume that the behavior that precedes the wave front must be undisturbed, so we conclude that  $z_{\text{exp}}$  is present only to the right of these points (the wake of the leading-order solitary wave). As we noted previously, more general nanopteron behavior can arise by relaxing this assumption, and that is one possible way to obtain two-sided nanoptera. However, modeling a wave front moving through an undisturbed chain necessitates that the region preceding the wave front contains no oscillatory behavior.

In Appendix 3.3, we use the form of the late-order terms in equation (3.21), truncate the asymptotic series, and determine the behavior that switches on as we cross a Stokes curve. The contribution associated with  $r = 2, 4$  is the complex conjugate of that associated with  $r = 1, 3$ , and we find that the form exponentially small contribution to the asymptotic behaviour in the wake of the solitary-wave is given by

$$z_{\text{exp}} \sim \left[ \frac{\mathcal{S}_1 \Lambda_1 \pi i \epsilon^{1/20}}{\sqrt{\chi_1'(\xi)}} e^{-\chi_1(\xi)/\sqrt{\epsilon}} + \frac{\mathcal{S}_3 \Lambda_3 \pi i \epsilon^{1/20}}{\sqrt{\chi_3'(\xi)}} e^{-\chi_3(\xi)/\sqrt{\epsilon}} \right] + \text{c.c.}, \quad \epsilon \rightarrow 0, \quad (3.23)$$

where ‘‘c.c.’’ stands for the complex conjugate, and  $\mathcal{S}_r$  varies from  $\mathcal{S}_r = 0$  on the side of the Stokes curve where  $\text{Im}(\chi_r) < 0$  to  $\mathcal{S}_r = 1$  on the side of the Stokes curve where  $\text{Im}(\chi_r) > 0$ . This variation occurs smoothly within a narrow neighborhood of width  $\mathcal{O}(\epsilon^{1/4})$  about the Stokes curve. (We show this calculation in detail in Appendix 3.3.) The expression in equation (3.23) simplifies to give

$$z_{\text{exp}} \sim 2\mathcal{S}_1 \pi \epsilon^{1/20} \text{Re} \left[ \frac{\Lambda_1}{\sqrt{\chi_1'}} \right] e^{-\text{Re}(\chi_1)/\sqrt{\epsilon}} \sin \left( \frac{\text{Im}(\chi_1)}{\sqrt{\epsilon}} \right) + 2\mathcal{S}_3 \pi \epsilon^{1/20} \text{Re} \left[ \frac{\Lambda_3}{\sqrt{\chi_3'}} \right] e^{-\text{Re}(\chi_3)/\sqrt{\epsilon}} \sin \left( \frac{\text{Im}(\chi_3)}{\sqrt{\epsilon}} \right), \quad \epsilon \rightarrow 0. \quad (3.24)$$

In Figure 3.2(c), we show an example of this behavior for  $\epsilon = 0.2$ ,  $\alpha = 1$ , and  $\kappa = 1$ . We

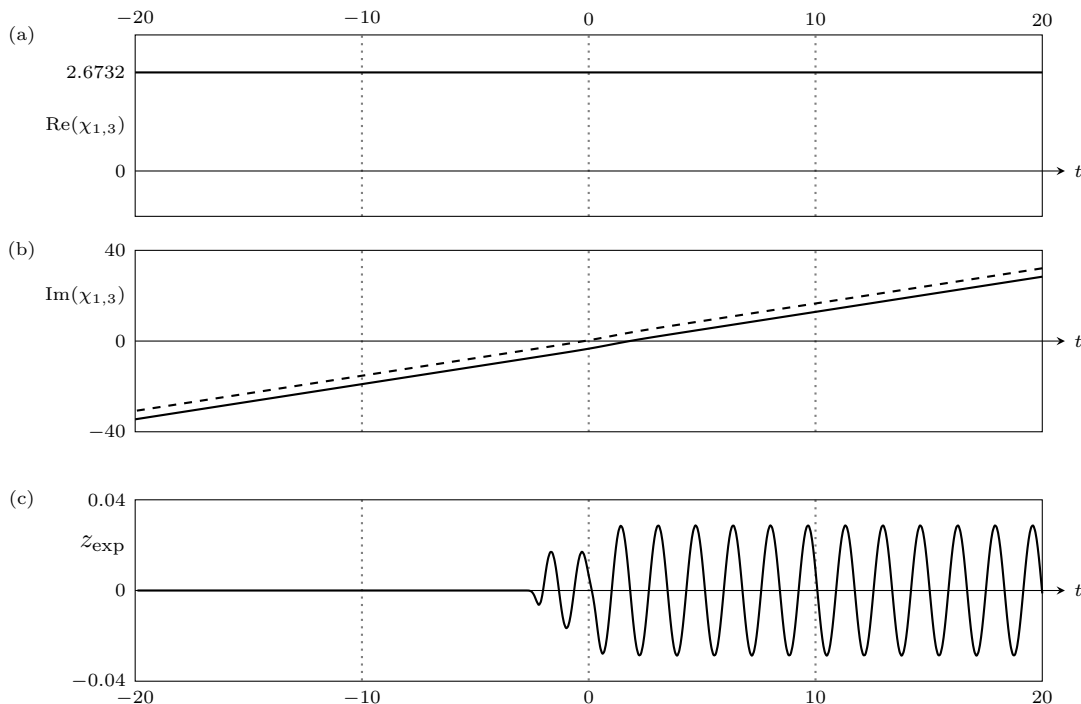


Fig. 3.2: We show the (a) real and (b) imaginary parts of  $\chi_{1,3}$  for a solitary wave traveling from left to right in  $n$  as  $t$  increases. We show  $\chi_1$  using a solid curve, and we show  $\chi_3$  using a dashed curve. The two singulants have identical real part. Panel (c) illustrates the exponentially small contribution  $z_{\text{exp}}$  that is switched across the Stokes curve. Observe that the exponentially-small contribution  $z_{\text{exp}}$  switches on at points satisfying  $\text{Im}(\chi_{1,3}) = 0$  and that it is present in the wake of the wave front located at  $t \approx 0$ .

see that oscillatory behavior is activated as the Stokes curve, which follows  $\text{Im}(\chi_{1,3}) = 0$ , is crossed. The remainder term  $z_{\text{exp}}$  consists of the sum of two oscillatory tails that do not decay in amplitude. In Figure 3.2, we see that these two contributions produce constructive interference when summed, so the wave train has a larger amplitude than the contributions associated with  $\chi_1$  or  $\chi_3$  individually.

Interference need not always be constructive, and in particular there exist values of  $\alpha$ ,  $\kappa$ , and  $\epsilon$  that produce destructive interference. Because the two oscillatory wave trains described in equation (3.24) have identical amplitudes, it is even possible to select parameter values so that the waves precisely cancel each other out. In Figure 3.3, we illustrate the asymptotic prediction of the oscillation amplitude with  $\alpha = 1$  and  $\kappa = 1$  for several values of the small mass ratio  $\epsilon$ . In the figure, we observe one particular mass ratio ( $\epsilon \approx 0.1304$ ) for which the amplitude disappears. This value produces two oscillatory tails that are exactly out of phase, leading to cancellation of the two wave trains. This configuration therefore produces a truly localized solitary wave, even at exponentially small orders. This behavior is consistent with the phenomenon of “resonance” in diatomic granular chains, discussed in [35], for which a particular discrete set of mass ratios produces special symmetries in the system that prevent nanoptera and instead produce a family of localized solitary waves.

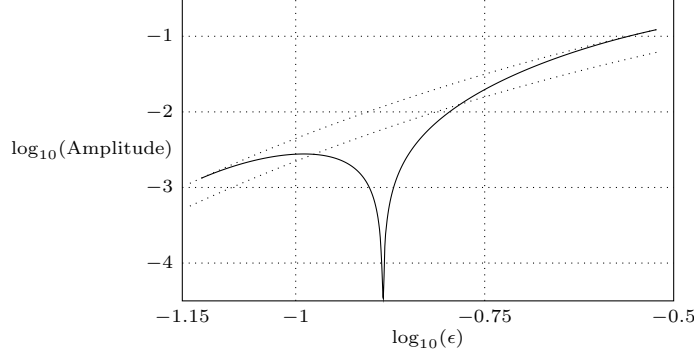


Fig. 3.3: Amplitude of the far-field oscillations given by the remainder expression  $z_{\text{exp}}$  in (3.24) with  $\alpha = 1$  and  $\kappa = 1$ . These oscillations are present in the wake of the traveling wave front. This expression contains two wave trains of equal amplitude. The lower dotted line indicates the individual amplitude of one oscillation, and the upper dotted line indicates the amplitude of the two oscillations if they were to interfere constructively (that is, twice the individual amplitude). There are regions at each end of the figure in which the two wave trains interfere constructively, and there is a region in the center in which the wave trains cancel each other out, resulting in a total amplitude that is much smaller than that of the individual wave trains. There is also one particular mass ratio ( $\epsilon \approx 0.1304$ ) in which the two waves are exactly out of phase, and they cancel precisely at that ratio.

We show in Appendix 3.3 using equation (C.19) that the exponentially-small contribution to the solution for  $y$  is

$$y_{\text{exp}} \sim -\frac{\epsilon}{2} \left[ \frac{\mathcal{S}_1(\xi-1)\Lambda_1\pi i\epsilon^{1/20}}{\sqrt{\chi'_1(\xi-1)}} e^{-\chi_1(\xi-1)/\sqrt{\epsilon}} + \frac{\mathcal{S}_3(\xi-1)\Lambda_3\pi i\epsilon^{1/20}}{\sqrt{\chi'_3(\xi-1)}} e^{-\chi_3(\xi-1)/\sqrt{\epsilon}} \right] - \frac{\epsilon}{2} \left[ \frac{\mathcal{S}_1(\xi)\Lambda_1\pi i\epsilon^{1/20}}{\sqrt{\chi'_1(\xi)}} e^{-\chi_1(\xi)/\sqrt{\epsilon}} + \frac{\mathcal{S}_3(\xi)\Lambda_3\pi i\epsilon^{1/20}}{\sqrt{\chi'_3(\xi)}} e^{-\chi_3(\xi)/\sqrt{\epsilon}} \right] + \text{c.c.}, \quad \epsilon \rightarrow 0, \quad (3.25)$$

which simplifies to a sinusoidal form similar to the one in equation (3.24). The amplitude of waves in the solution for  $y$  is smaller than those in  $z$  by a factor of  $\epsilon$ .

The value  $\chi'_s(\xi)$  tends to a constant value in the far field (i.e., in the limit that  $\xi \rightarrow \infty$ ). Because  $y_0(\xi) - y_0(\xi+1) \rightarrow 0$  as  $\xi \rightarrow \infty$ , we see that  $\lambda[(\chi'_s)^2] \rightarrow -2$  in this limit and consequently that  $\chi'_s$  tends to a constant value. In Figure 3.2, we see that  $\text{Im}(\chi_s) > 0$  for large  $\xi$  and hence that  $\chi'_s \rightarrow i\sqrt{2/\lambda}$ . Consequently, the amplitude of the waves in equation (3.24) tends to a constant value as  $\xi \rightarrow \infty$ .

**4. Numerical Comparison.** To verify our approximation, we compare the far-field amplitude (i.e., as  $\xi \rightarrow \infty$ ) of the waves predicted by equation (3.24) with a numerical simulation of the nonlocal solitary waves for particular choices of soliton parameters.

We discretize the time domain with a time step of  $\Delta t$ , which we choose to be sufficiently small to capture oscillations with wavelength  $\mathcal{O}(\sqrt{\epsilon})$ . We thus need  $\Delta t \ll \sqrt{\epsilon}$ . The spatial variable is already discrete, and we apply domain bounds of  $-n_\infty \leq n \leq n_\infty$ , where  $n_\infty$  is sufficiently large

that boundary effects never interact with the solitary waves. In practice, we set  $n_\infty > 2ct_{\max}$ , where  $c$  is the speed of the leading-order solitary wave and  $t_{\max}$  is the maximum time of the simulation. Because the solution decays exponentially ahead of the wave front at leading order, this ensures that the wave front and its effects are never near enough to the boundary for boundary effects to influence the wave behavior.

We also need initial conditions for the solution and its time derivative at  $t = 0$ . To obtain these, we use the leading-order behavior in equations (3.12,3.13) evaluated at  $t = 0$ . This gives initial values for  $y(n, 0)$  and  $z(n, 0)$  of

$$y(n, 0) = y_+ + \log \left( \frac{1 + \alpha \exp(-2\kappa n)}{1 + \alpha \exp(-2\kappa(n+1))} \right), \quad (4.1)$$

$$z(n, 0) = y_+ + \frac{1}{2} \log \left( \frac{1 + \alpha \exp(-2\kappa n)}{1 + \alpha \exp(-2\kappa(n+2))} \right). \quad (4.2)$$

By evaluating the time derivative of this leading-order behavior at  $t = 0$  and applying a first-order forward difference, we assign values for  $y(n, \Delta t)$  and  $z(n, \Delta t)$  of

$$y(n, \Delta t) = y(n, 0) + \Delta t \dot{y}_0(n, 0), \quad z(n, \Delta t) = z(n, 0) + \Delta t \dot{z}_0(n, 0), \quad (4.3)$$

where we recall that  $\dot{\cdot}$  indicates a derivative with respect to time. Finally, we specify boundary conditions on  $n$  such that  $y(n_\infty, t) = y(n_\infty, 0)$  and  $z(n_\infty, t) = z(n_\infty, 0)$ , ensuring that the boundary values are consistent with the initial conditions. We choose the value of  $n_\infty$  to be sufficiently large to be able to treat  $z(\pm n_\infty, t)$  as constant, as the wave front in the solution never goes near  $n = n_\infty$ . In our simulations, we choose the value of  $n_\infty$  to be more than twice the distance traveled by the wave front (which moves with a velocity of  $\sinh(\kappa)/\kappa\sqrt{2}$ ).

We use a numerical scheme with a second-order central-difference discretization for the continuous time derivatives in the governing equations. At each time step, we construct a nonlinear system of equations using a MATLAB built-in nonlinear system solver (FSOLVE), which utilizes a variant of the Powell dogleg procedure described in detail in [58].

In Figure 4.1(a), we illustrate  $z(n, t)$  calculated using the parameter values  $\epsilon = 0.2$ ,  $y_+ = 0$ ,  $\kappa = 1$ , and  $\alpha = 1$ . As expected, there is a wave front that travels in the positive direction, with radiation that travels in the negative direction. We are interested in the oscillations that immediately follow the solitary-wave front.

We show the exponentially small oscillations in more detail in Figure 4.1(b), in which we restrict the shading to a narrower range. This region, which corresponds to the region in Figure 4.1(a) that is surrounded by a white rectangle, contains visible oscillations that follow in the wake of the solitary wave front without decaying. Additionally, the solution along the dashed line in Figure 3.1, following  $n = 30$ , is shown in detail in Figure 3.1.

In Figure 4.2, we compare the asymptotic approximation with the numerical approximation for several values of the mass ratio  $\epsilon$  using the parameter values  $y_+ = 0$ ,  $\kappa = 1$ , and  $\alpha = 1$ . We compare the amplitude predicted by the asymptotic analysis versus the computed amplitude in panel (a), and we compare the wavelengths in panel (b). For values of  $\epsilon$  that are larger than the

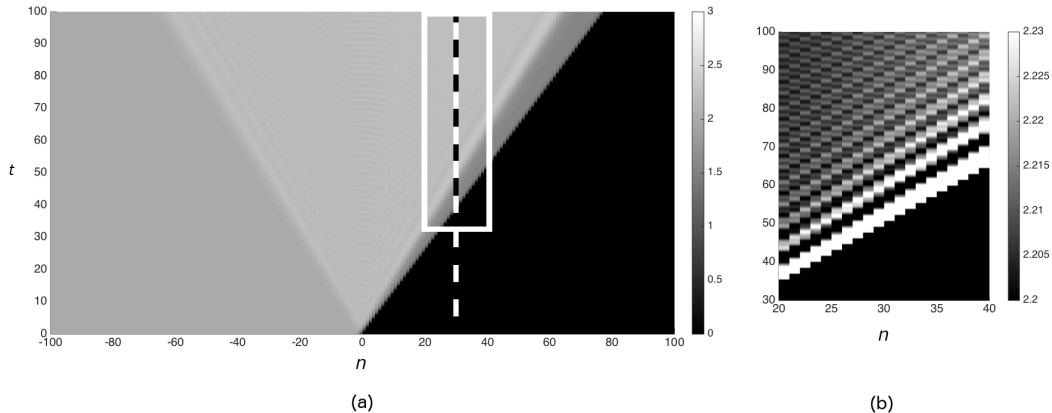


Fig. 4.1: (a) Behavior of  $z(n, t)$  for  $\epsilon = 0.2$ . The initial condition of the simulation is given by the leading-order dynamics, which we show in equations (3.12,3.13). The wave front originates at  $n = 0$  and propagates from left to right. There are also visible effects on the  $\mathcal{O}(\epsilon)$  scale that propagate outwards from the point  $n = 0$ . (b) A magnification of the region in the white rectangle. In this region, the large-scale transient effects dissipate, but small and non-decaying oscillations trail behind the wave front. These oscillations are examples of the exponentially-small nanopteron behavior. In Figure 3.1, one can observe the solution across the dashed line in panel (a).

depicted ones, the asymptotic approximation (3.24) becomes inaccurate. For values of  $\epsilon$  that are smaller than the depicted ones, it becomes difficult to compute the waves numerically, because the amplitude decays exponentially in  $\epsilon$ .

Note that the exponentially small contribution to the solution in (3.24) is the sum of two wave contributions of identical amplitude but different phase. From Figure 3.3, we see that there are some values of  $\epsilon$  in which these waves interfere constructively and other values in which they interfere destructively. Our asymptotic analysis also predicts that there are values of  $\epsilon$  for which the waves precisely cancel out (in this case, for  $\epsilon \approx 0.1304$ ). However, the numerical results in Figure 4.2 suggest that this cancellation occurs at  $\epsilon \approx 0.12$ . Calculating amplitudes for values of  $\epsilon$  nearer to 0.12 become prohibitively difficult with the present numerical scheme due to the small magnitude of the oscillations in the solution.

For the values of the mass ratio  $\epsilon$  in Figure 4.2, the asymptotic expression (3.24) can provide an accurate prediction of both (1) the far-field amplitude, which decays exponentially in  $\epsilon$ , and (2) the oscillation wavelength, which decays as  $\epsilon^{1/2}$  in the  $\epsilon \rightarrow 0$  limit. However, our prediction for the amplitude becomes significantly less accurate for very small values of  $\epsilon$ , although it does follow the correct qualitative trend. Even for these cases, the accuracy of the predicted wavelength does not deteriorate.

It is likely that the reason for our inaccurate quantitative prediction of the amplitude for very small  $\epsilon$  arises from unaccounted destructive interference between the two wave trains. As the wavelength becomes small (in particular, for  $\mathcal{O}(\sqrt{\epsilon})$  as  $\epsilon \rightarrow 0$ ), asymptotic approximation error on this scale in the phase of oscillations can lead to significant differences in the interference

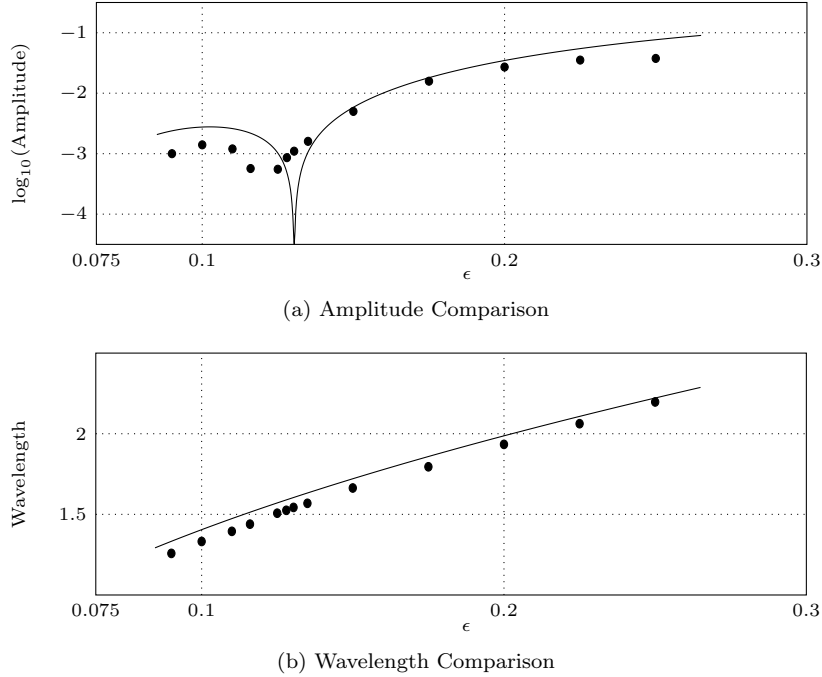


Fig. 4.2: Comparison of asymptotic prediction of (a) nanopterion amplitude and (b) nanopterion wavelength. We indicate our asymptotic predictions (3.24) by a solid curve, and we indicate numerically-calculated values with black dots. In these simulations, we use initial conditions given by a leading-order wave with mass ratio  $\epsilon$  and fixed parameter values  $\kappa = 1$  and  $\alpha = 1$ . The observed dynamics arises from the sum of two wave trains of identical amplitude but different phase, and we therefore obtain constructive interference at some parameter values and destructive interference at others. Our asymptotic approximation for the amplitude is qualitatively consistent with the numerical solutions, although there is a discrepancy between the asymptotic and computational results when  $\epsilon$  becomes too small. We do not observe such a discrepancy in the asymptotic approximation for the wavelength, which shows good agreement with the computational results for all of the tested values of  $\epsilon$ . This suggests that the error is due to small asymptotic errors in the phase of the oscillations. This oscillatory terms in the solution have very small wavelengths, so small phase shifts can produce significant differences in interaction effects (such as destructive interference). From (3.24), we see that the two wave trains have identical wavelengths at the asymptotic order that we consider. Therefore, their sum has the same wavelength — independent of phase — so phase errors do not affect the wavelength, which is consistent with the results in panel (b).

effects between the asymptotic predictions and computed results. However, at the order computed, the two wave trains have identical wavelengths, ensuring that the sum of the two wave trains also has the same wavelength for any phase. Consequently, phase errors have no effect on the wavelength of the oscillations at the order computed in (3.24). We see in Figure 4.2(b) that there is agreement between the predicted and computed wavelengths, even for values of  $\epsilon$  in which the wave-train interactions cause our amplitude calculations to be inaccurate quantitatively. This suggests that small errors in the phase of the oscillation are the cause of the inaccuracy in the amplitude predictions for very small  $\epsilon$ .

Taking into account the issues with the asymptotic predictions of amplitude, it is still apparent

that our asymptotic analysis is capable of providing useful qualitative descriptions of the wave behavior, and it accurately predicts the wavelength of the oscillations. There is some disagreement between our asymptotic prediction and numerical calculations of the oscillation amplitude for particularly small values of  $\epsilon$ , and the exact value of  $\epsilon$  for which wave cancellation occurs, but these values still possess a reasonable qualitative agreement. Figure 4.2(a) indicates that the asymptotic amplitude predictions are useful provided the value of  $\epsilon$  is not so small that it becomes difficult to accurately account for interaction effects between wave trains.

**5. General Nearest-Neighbor Systems.** As we noted in Section 1, a Toda lattice is a special case of a general model of a chain of particles with nearest-neighbor interactions. By selecting a different interaction potential, one can consider other systems on a periodic lattice.

We consider a general class of nearest-neighbor interactions with the form

$$\ddot{y}(n, t) = f(z(n-1, t) - y(n, t)) - f(y(n, t) - z(n, t)) , \quad (5.1)$$

$$\epsilon \ddot{z}(n, t) = f(y(n, t) - z(n, t)) - f(z(n, t) - y(n+1, t)) , \quad (5.2)$$

where we recall that a dot indicates a derivative with respect to time.

We assume that the system (5.1,5.2) has a solitary-wave solution when  $\epsilon = 0$  (such as the solitary-wave solutions in (3.13)), and that this solution contains at least one pair of singularities in the analytic continuation of time  $t$ . The pair of singularities nearest to the real axis are located at  $t = t_s$  and its complex conjugate  $t = \bar{t}_s$ . In this case, we analytically continue  $t$ , while treating  $n$  as a parameter in the problem.

By expanding  $y(n, t)$  and  $z(n, t)$  as an asymptotic power series, as in equation (3.8), we match powers of  $\epsilon$  to determine expressions for the series coefficients  $y_j(n, t)$  and  $z_j(n, t)$ . At leading order, we find that

$$z_0(n, t) = \frac{1}{2} (y_0(n, t) + y_0(n+1, t)) . \quad (5.3)$$

At subsequent orders, we obtain

$$\begin{aligned} \ddot{y}_j(n, t) &= f'(z_0(n-1, t) - y_0(n, t)) (z_j(n-1, t) - y_j(n, t)) \\ &\quad - f'(y_0(n, t) - z_0(n, t)) (y_j(n, t) - z_j(n, t)) , \end{aligned} \quad (5.4)$$

$$\begin{aligned} \epsilon \ddot{z}_{j-1}(n, t) &= f'(y_0(n, t) - z_0(n, t)) (y_j(n, t) - z_j(n, t)) \\ &\quad - f'(z_0(n, t) - y_0(n+1, t)) (z_j(n, t) - y_j(n+1, t)) . \end{aligned} \quad (5.5)$$

Applying a late-order ansatz of the form (3.16) to the recursion relations (5.4) and simplifying the expression yields an expression for the singulant equation, which we can simplify using the relationship (5.3) between the leading-order terms  $y_0$  and  $z_0$  to give

$$[\dot{\chi}(n, t)]^2 = -2f' \left( \frac{1}{2}(y_0(n+1, t) - y_0(n, t)) \right) , \quad (5.6)$$

with  $\chi = 0$  at  $t = t_s$  or at  $t = \bar{t}_s$ . As with the Toda lattice, the singulant is  $Z(n, t) = \Lambda/\sqrt{\dot{\chi}(n, t)}$ , where  $\Lambda$  is a constant to be determined using the methods in Appendix B.2.

To determine the singulant  $\chi$ , we need global information about  $y_0$  in the complex plane. We can then solve equation (5.6) by numerical integration to gain information about the exponentially-small asymptotic behaviour in the system. The singulant associated with the singularity at  $t = t_s$  is

$$\chi = \pm i\sqrt{2} \int_{t_s}^t \sqrt{f' \left( \frac{1}{2}(y_0(n+1, s) - y_0(n, s)) \right)} ds. \quad (5.7)$$

Equation (5.7) allows one to determine a condition that must be satisfied for the solution of (5.1,5.2) to contain a non-decaying wave train of constant amplitude that switches on across a Stokes curve. The quantity that switches on as the Stokes curve is crossed takes the form  $R_N \sim AZe^{-\chi/\sqrt{\epsilon}} + \text{c.c.}$  as  $\epsilon \rightarrow 0$ . The Stokes curve satisfies  $\text{Re}(\chi) > 0$  and  $\text{Im}(\chi) = 0$ , ensuring that this quantity is exponentially small.

For a non-decaying downstream wave train to exist, we need for fixed  $n$  that

$$f' \left( \frac{1}{2}(y_0(n+1, t) - y_0(n, t)) \right) \rightarrow k \quad \text{as } t \rightarrow \infty, \quad (5.8)$$

where  $k$  is some real, positive constant. This ensures that  $\dot{\chi} \sim \pm i\sqrt{2k}$  in the  $t \rightarrow \infty$  limit and that the prefactor  $Z$  tends to a constant value in this limit. If  $k$  is real and positive, the exponential term in  $R_N$  does not decay or grow as  $\xi \rightarrow \infty$ , so the wave train described by the remainder term is purely oscillatory. In this case, for fixed  $n$ , one obtains

$$R_N \sim 2AZ_\infty e^{-\chi_R/\sqrt{\epsilon}} \cos \left( \sqrt{\frac{2k}{\epsilon}} t \right) \quad \text{as } t \rightarrow \infty, \quad (5.9)$$

where  $A$  is a constant,  $Z_\infty$  is a constant that is determined by the behavior of  $Z(n, t)$  in the  $t \rightarrow \infty$  limit, and the constant  $\chi_R$  is the real part of  $\chi$  as  $t \rightarrow \infty$ . Consequently, the asymptotic solution contains exponentially-small waves of constant amplitude (i.e., nanoptera) extending backwards from the wave front, and we can determine the behavior of these nanoptera using the method that we discussed in Section 3.

We assumed that the leading-order solution  $y_0$  is a solitary wave, which we obtained by solving (5.1,5.2) with  $\epsilon = 0$ . Hence, we note that  $y_0(n+1, t) - y_0(n, t) \rightarrow 0$  for fixed  $n$  as  $t \rightarrow \infty$ . We can thus simplify the requirement (5.8) to

$$f'(0) > 0. \quad (5.10)$$

For the Toda lattice,  $f(s) = e^{-s}$ , so  $f'(0) = 1$ .

The condition (5.10) allows us to draw conclusions about the existence of non-decaying wave trains in general periodic systems governed by nearest-neighbor interactions. For example, consider a lattice equation for chains with a two-sided power-law contact force and without precompression. (A one-sided version of such a chain is a granular chain [50, 62].) In this case,

$f(s) = s^\nu$ , so

$$\ddot{y}(n, t) = [z(n-1, t) - y(n, t)]^\nu - [y(n, t) - z(n, t)]^\nu, \quad (5.11)$$

$$\epsilon \ddot{z}(n, t) = [y(n, t) - z(n, t)]^\nu - [z(n, t) - y(n+1, t)]^\nu, \quad (5.12)$$

where the choice of  $\nu$  indicates the nature of the interaction between particles. The Hertzian case  $\nu = 3/2$  is particularly noteworthy [50, 62], and we henceforth consider the case  $\nu = 3/2$ .

The analogous monoatomic chain contains solitary-wave solutions, from which one can construct solutions to the  $\epsilon = 0$  case of the period-2 system in the same fashion as in our analysis of the period-2 Toda lattice. Pego and English [25] gave a method for constructing solitary-wave solutions in terms of an integral equation, and [63] provided the first few terms of a convergent approximation to the solitary-wave solution.

An example approximate solitary-wave solution for the  $\epsilon = 0$  system constructed by taking the first few terms of this convergent approximation is

$$y_0(\xi) = -2 \tanh \left[ \frac{1}{2} (C_1 \xi + C_3 \xi^3 + C_5 \xi^5) \right], \quad z_0(\xi) = \frac{1}{2} [y_0(\xi) + y_0(\xi + 1)], \quad (5.13)$$

where  $\xi = n - \sqrt{2C_0}t$ , with  $C_0 \approx 0.85852$ ,  $C_1 \approx 2.39536$ ,  $C_3 \approx 0.268529$ , and  $C_5 \approx 0.0061347$ .

Using the approximation (5.13) as a leading-order solution, we see that there exist poles in the analytic continuation of  $\xi$  located at solutions to  $C_1 \xi + C_3 \xi^3 + C_5 \xi^5 = M\pi i$ , where  $M$  is an odd integer. The relevant singularities of the leading-order behavior of equation (5.13) are located at  $\xi \approx \pm 0.498 + 1.856i$  and their associated complex conjugates. Consequently, the system satisfies the required assumptions on the leading-order behavior.

If  $f(s) = s^{3/2}$ , it follows that  $f'(0) = 0$ , so although an exponentially small contribution is present in the asymptotic solution due to Stokes curve associated with  $\chi$ , there are no oscillations in the wake of the wave front. See Figure 5.1(c), where we illustrate that the quantity  $e^{-\chi/\sqrt{\epsilon}}$  tends to a constant value, rather than producing the oscillatory behavior observed in Figure 3.2(c). Recalling that  $R_N \sim AZe^{-\chi/\sqrt{\epsilon}}$ , we conclude that the exponentially small contribution associated with the Stokes curve corresponds to an offset, in contrast to the oscillations of non-decaying amplitude that we obtained in the Toda case.

The singulant calculated using equation (5.6) tends to a complex constant in the far field (i.e., as  $\xi \rightarrow \infty$ ), as we illustrate in Figure 5.1. Consequently, although the solution contains an exponentially-small contribution that switches on across a Stokes curve, the phase of this contribution tends to a constant value once temporal effects have settled. One can observe this clearly in Figure 5.1, where the phase varies near  $\xi = 0$  but subsequently settles and is effectively constant beyond  $\xi \approx 5$ .

**6. Discussion and Conclusions.** In this study, we derived asymptotic solutions to singularly-perturbed period-2 discrete particle systems governed by nearest-neighbor interactions in which the leading-order solution is a solitary wave. These solutions exhibit a particular feature, known as nanoptera, in which the solitary-wave solution is not localized but instead contains non-

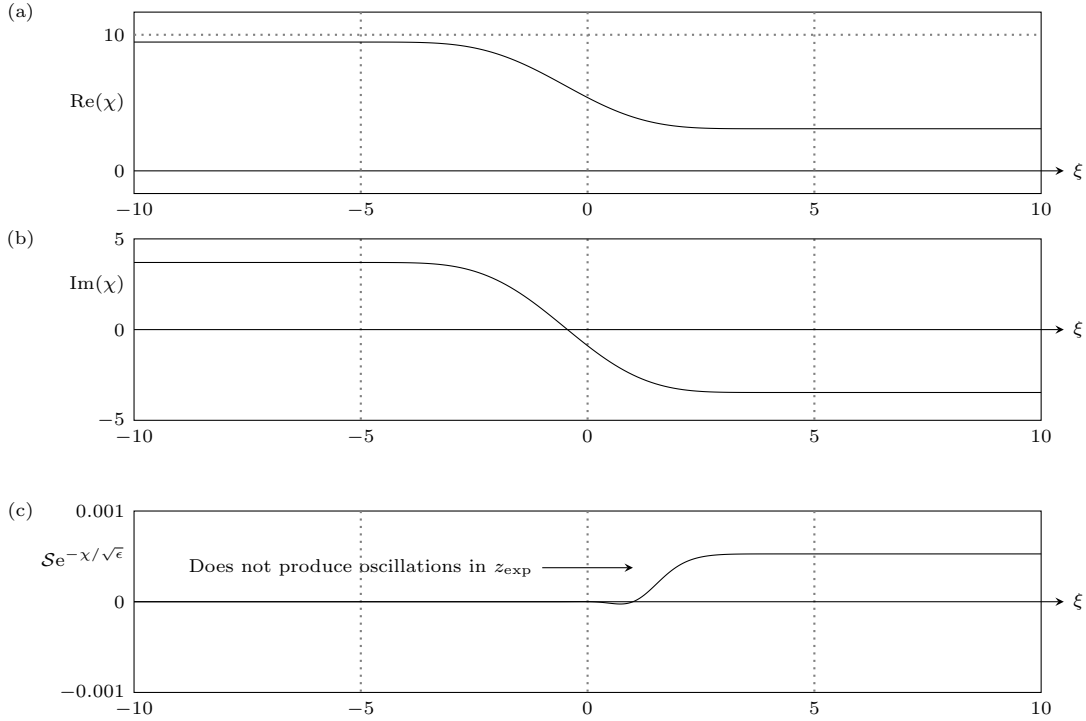


Fig. 5.1: (a) Real and (b) imaginary parts of the singulant  $\chi$  associated with a solitary wave in a period-2 chain of with a two-sided  $3/2$  power-law nearest-neighbor interaction with leading-order behavior (5.13). Panel (c) illustrates  $\mathcal{S}e^{-\chi/\sqrt{\epsilon}}$  with  $\epsilon = 0.2$ . As in a period-2 Toda lattice, one crosses a Stokes curve at the point satisfying  $\text{Im}(\chi) = 0$ . Crossing the Stokes curve switches on a contribution proportional to  $\mathcal{S}e^{-\chi/\sqrt{\epsilon}}$ . However, in the wake of the wave front, the phase function  $\chi$  tends to a constant value (i.e.,  $\chi'(\xi) \rightarrow 0$ ) as  $\xi \rightarrow \infty$ . Therefore, although an exponentially-small contribution is switched on across the Stokes curve, it does not contain non-decaying oscillations. This contrasts with our observation for the period-2 Toda lattice.

decaying trains of oscillations in the wake of the wave front. These oscillations are exponentially small, so their dynamics are invisible to ordinary asymptotic power series approaches. Using exponential asymptotic methods, we derived asymptotic descriptions of these oscillations in the singularly-perturbed limit.

In the first part of our study, we applied exponential asymptotics to determine the asymptotic behavior of solitary waves in a period-2 Toda chain. We found that the solutions contain exponentially small oscillations in the wake of the solitary wave front and that the amplitude of these oscillations tends to a constant value away from the front, and we obtained an asymptotic expression (3.24,3.25) for these oscillations.

By examining (3.24), we found that there exist system configurations in which the wave trains cancel entirely (see Figure 3.3). In this case, the solutions do not possess a wave train in the wake of the solitary wave front; instead, they contain a localized solitary wave. This is reminiscent of the results in [35, 37, 70], in which special choices of wave parameters and mass ratios produce purely localized solitary-wave solutions due to cancellation of the oscillatory tails. In particular, [35] showed numerically that wave cancellation can occur in period-2 lattice

systems, and [36] showed that constructive interference can also be produced by configurations in which the two wave trains are precisely in phase. Our asymptotic study provides another perspective on such dynamics.

We compared the asymptotic expressions for the nanoptera to numerical simulations of the period-2 Toda system, and we found that the results are qualitatively consistent with each other. For sufficiently small  $\epsilon$ , however, the asymptotic approximations predict the amplitude of the oscillations inaccurately. Our prediction for the oscillation wavelength remains accurate in this regime; this suggests that the error in the amplitude arises from interactions between the two wave trains. In particular, because of the short wavelength of the oscillations (they are  $\mathcal{O}(\sqrt{\epsilon})$  as  $\epsilon \rightarrow 0$ ), small errors in the phase would cause the interference effects between the two wave trains in the solution to be approximated incorrectly, significantly affecting the predicted amplitude but not the predicted wavelength. This phase error is also responsible for slightly changing the value of  $\epsilon$  for which the oscillations cancel entirely.

We subsequently considered solitary-wave solutions to a general form of singularly-perturbed period-2 systems in (5.1,5.2). Using a similar method as in the first part of our study, we derived equation (5.7) for the singulant, which governs the phase of the exponentially-small oscillations. From the singulant equation (5.7), we derived a simple criterion for the presence of exponentially-small nanopteron-type waves in the solution (5.10). Specifically, we found that if the analytic continuation of the leading-order solution contains singular points (and hence exhibits the Stokes phenomenon), then if  $f'(0)$  is real and non-negative, the solution contains exponentially small, non-decaying oscillations that switch on across a Stokes curve. These oscillations form the non-decaying oscillatory tail of a nanopteron that is centered on the solitary wave front. If this condition on  $f$  is not satisfied, an exponentially small contribution is still switched across the Stokes curve, and one can calculate the behavior of this contribution in a similar fashion to the exponential asymptotic calculations in Section 3.3. However, it is possible that this contribution will not contain oscillations, as one can see in Figure 5.1, or that it may contain nanoptera that decay exponentially in amplitude away from the wave front.

It would be very interesting to generalize our analysis to determine the behavior of solutions to more complicated 2-periodic particle chains that do not fall into the general form described in (5.1,5.2). In particular, a similar analysis could be applied to the woodpile system studied in [38]. This experimental study demonstrated that solitary-wave solutions in woodpile systems exhibit nanoptera, and that there exist discrete sets of special configurations in which the oscillatory wave trains cancel to produce localized wave fronts. This suggests that an exponential asymptotic analysis of this system should reveal similar results to those illustrated for the Toda lattice in Figure 3.3.

One can do similar analysis using  $N$ -soliton solutions of constant-mass lattice problems, such as the  $N$ -soliton solution (1.8) to the Toda lattice. It would be interesting to consider solutions to the associated singularly-perturbed periodic lattice systems and how the far-field oscillations are affected by the presence of multiple solitary wave fronts in the solution. It would be particularly interesting to determine whether one can generate solutions in which the two lead to the

cancellation of the oscillatory tails from the interaction of multiple solitary wave fronts.

The precise cancellation of exponentially-small downstream oscillations due to destructive interference is a key feature in [45], which studied the trapped surface waves for free-surface flow over a submerged bump or trench. In general, the two edges of the obstacle produce downstream surface waves. However, for particular choices of the step angle and fluid properties, it is possible to produce solutions in which the downstream waves cancel precisely, ensuring that the waves are “trapped” (i.e., localized) in the region between the two edges. Cancellation of exponentially small oscillations also occurs in [15], which obtained nanopteron solutions to a perturbed nonlinear Schrödinger equation in which a wave train is restricted to the region between solitary waves. It would be particularly interesting to see if “trapped-wave” solutions can also be produced for granular chains in which the oscillatory wave train is contained in the finite region between two solitary-wave fronts. This would be caused by the wave train from one wave front being cancelled precisely by the wave train from a following wave front.

Finally, extending the results of our study to singularly-perturbed periodic particle chains of higher periodicities does not require additional asymptotic techniques beyond those that we have used, although the analysis would be significantly more complicated. In particular, such analysis could involve a hierarchy of small parameters, depending on the mass ratios in the problem. Dynamical systems with two or more small parameters can produce a large variety of complicated behavior (see, e.g., [22]), and it would pose a fascinating challenge.

**Acknowledgements.** CJL thanks Prof. Nalini Joshi for helpful discussions. CJL was supported by Australian Laureate Fellowship Grant #FL120100094 from the Australian Research Council.

### Appendix A. Late-Order Term Calculations.

In this section, we determine the form of the late-order ansatz proposed in (3.16). As we discussed in Section 2, the late-order behavior takes the form of a sum of factorial-over-power terms, each of which is associated with a singularity in the leading-order behavior of  $z_0$  given by (3.13).

The leading-order behavior  $z_0$  is singular at points that satisfy

$$1 + \alpha \exp(-2\kappa\xi) = 0 \quad \text{or} \quad 1 + \alpha \exp(-2\kappa(\xi + 2)) = 0. \quad (\text{A.1})$$

Equations (A.1) have an infinite number of solutions, which are located at

$$\xi = \frac{1}{2\kappa} [\log \alpha + M\pi i], \quad \xi = \frac{1}{2\kappa} [\log \alpha + M\pi i] - 2, \quad (\text{A.2})$$

where  $M$  is any odd integer.

We restrict our attention to singularities with  $M = \pm 1$ , as these are closest to the real axis and hence dominate the far-field wave behavior. Furthermore, the exponentially-small contribution associated with  $M = -1$  is the complex conjugate of that associated with  $M = 1$ . Hence, we examine  $M = 1$  and subsequently add the appropriate complex-conjugate contribution to

account for  $M = -1$ . The four relevant singularities are

$$\xi_{1,2} = \frac{1}{2\kappa} (\log \alpha \pm \pi i), \quad \xi_{3,4} = \frac{1}{2\kappa} (\log \alpha \pm \pi i) - 2. \quad (\text{A.3})$$

Applying the late-order ansatz (3.16) to the first governing equation (3.14) shows that we need  $\gamma_1 + 2 = \gamma_2$  to obtain a nontrivial balance. This implies that  $y_r = \mathcal{O}(z_{r-1})$  and hence that  $z_r$  dominates  $y_r$  in the late-order recursion equations (3.14,3.15).

Applying the late-order ansatz (3.16) to the second governing equation (3.15) gives

$$\begin{aligned} & \frac{\lambda(\chi'(\xi))^2 Z(\xi) \Gamma(2j + \gamma_2)}{\chi(\xi)^{2j + \gamma_2}} - \frac{2\lambda\chi'(\xi)Z'(\xi)\Gamma(2j + \gamma_2 - 1)}{\chi(\xi)^{2j + \gamma_2 - 1}} \\ & - \frac{\lambda\chi''(\xi)Z(\xi)\Gamma(2j + \gamma_2 - 1)}{\chi(\xi)^{2j + \gamma_2 - 1}} = -2e^{-\frac{1}{2}(y_0(\xi+1) - y_0(\xi))} \frac{Z(\xi)\Gamma(2j + \gamma_2)}{\chi(\xi)^{2j + \gamma_2}} + \dots, \end{aligned} \quad (\text{A.4})$$

where the omitted terms are no larger than  $\mathcal{O}(z_{r-1})$  in the  $r \rightarrow \infty$  limit. We now equate terms that are  $\mathcal{O}(z_r)$  as  $r \rightarrow \infty$  to obtain the singular equation

$$\lambda [\chi'(\xi)]^2 = -2e^{-\frac{1}{2}[y_0(\xi+1) - y_0(\xi)]}, \quad \chi = 0 \quad \text{at} \quad \xi = \xi_s, \quad (\text{A.5})$$

where  $\xi_s$  is the location of the singularity under consideration. For  $M = \pm 1$ , we give the location in (A.2).

We now match equation (A.4) at the next order in  $j$  by equating terms of  $\mathcal{O}(z_{r-1/2})$  as  $r \rightarrow \infty$ . This yields the equation

$$2Z'(\xi)\chi'(\xi) + Z(\xi)\chi''(\xi) = 0 \quad (\text{A.6})$$

for the prefactor  $Z$ . We then integrate (A.6) to obtain

$$Z(\xi) = \frac{\Lambda}{\sqrt{\chi'(\xi)}}, \quad (\text{A.7})$$

where  $\Lambda$  is a constant that one can determine by considering the behavior of the solution near  $\xi = \xi_s$  and comparing it to the leading-order behavior in this local neighborhood. We perform this local analysis in Appendices B.1 and B.2.

In Appendix B.1, we show that the late-order ansatz is consistent with the leading-order behavior in the neighborhood of the singularity at  $\xi = \xi_s$  only when  $\gamma_2 = -1/10$ . In Appendix B.2, we compute  $\Lambda$  numerically to obtain the constant values  $\Lambda_{1,2} = -0.3500\sqrt{\beta}$  and  $\Lambda_{3,4} = -0.3500\sqrt{\beta}$ , where

$$\beta \approx i \left[ \frac{2\sqrt{2\kappa}}{\lambda} \sqrt{\frac{e^{2\kappa} + 1}{e^{2\kappa} - 1}} \right]^{1/2}. \quad (\text{A.8})$$

## Appendix B. Local Analysis Near the Singularity.

**B.1. Determining  $\gamma_2$ .** To determine  $\gamma_2$  and  $\Lambda$ , we need to consider the behavior of the solution near the singularity under consideration, where the asymptotic series (3.8) breaks down. To determine the correct scaling, we examine the local behavior of  $y_0$  and  $z_0$  and hence of  $\chi$ . In our analysis, we consider the first case from (A.2) with  $M = 1$ , for which the location of the singularity  $\xi_1$  is

$$\xi_s = \frac{1}{2\kappa} [\log \alpha + \pi i]. \quad (\text{B.1})$$

Using the expressions (3.13) for  $y_0$  and  $z_0$ , we find near  $\xi = \xi_s$  that

$$y_0(\xi) = \log(\xi - \xi_s) + [y_+ + \log(2\kappa) - \log(1 - e^{-2\kappa})] + \mathcal{O}(\xi - \xi_s), \quad (\text{B.2})$$

$$z_0(\xi) = \frac{1}{2} \log(\xi - \xi_s) + [y_+ + \frac{1}{2} \log(2\kappa) - \frac{1}{2} \log(1 - e^{-4\kappa})] + \mathcal{O}(\xi - \xi_s), \quad (\text{B.3})$$

$$y_0(\xi + 1) = y_+ - \log(1 + e^{-2\kappa}) + \mathcal{O}(\xi - \xi_s). \quad (\text{B.4})$$

Using the singulant equation (A.5) in conjunction with equations (B.2) and (B.4), we obtain

$$\chi' \sim i \left[ \frac{2\sqrt{2\kappa}}{\lambda} \sqrt{\frac{e^{2\kappa} + 1}{e^{2\kappa} - 1}} \right]^{1/2} (\xi - \xi_s)^{1/4} \quad \text{as} \quad \xi \rightarrow \xi_s. \quad (\text{B.5})$$

Integrating (B.5) yields

$$\chi \sim \frac{4\beta}{5} (\xi - \xi_s)^{5/4}, \quad (\text{B.6})$$

where

$$\beta = i \left[ \frac{2\sqrt{2\kappa}}{\lambda} \sqrt{\frac{e^{2\kappa} + 1}{e^{2\kappa} - 1}} \right]^{1/2}.$$

Consequently, the local behavior of the factorial-over-power ansatz (3.16) is

$$z_j(n, t) \sim \frac{\Lambda \Gamma(2j + \gamma_2)}{\sqrt{\beta} (\xi - \xi_s)^{1/4} \left[ \frac{4\beta}{5} (\xi - \xi_s)^{5/4} \right]^{2j + \gamma_2}} \quad \text{as} \quad \xi \rightarrow \xi_s. \quad (\text{B.7})$$

For (B.7) to be consistent with the leading-order behavior (3.13), which has a logarithmic singularity, we require that the strength of the singularity is equal to 0 (i.e., that it is logarithmic) when  $r = 0$ . It then follows that  $1/8 + 5\gamma_2/4 = 0$ , which gives  $\gamma_2 = -1/10$ .

**B.2. Determining  $\Lambda$ .** From equation (3.16), we see that the factorial-over-power ansatz breaks down when  $\epsilon \chi^{-2} = \mathcal{O}(1)$  as  $\epsilon \rightarrow 0$ . Therefore, we define the inner scaling  $\xi - \xi_s = \epsilon^{2/5} \bar{\xi}$ . We must consider the local expansion of the leading-order singular behavior in a neighborhood about  $\xi = \xi_s$  of radius  $\mathcal{O}(\epsilon^{2/5})$  as  $\epsilon \rightarrow 0$ , and we then match it with the outer ansatz. Because we are interested in the divergent behavior of the solution associated with the singular perturbation

$z$ , we express  $z_0$  in terms of the inner variables and rescale to obtain

$$y(\bar{\xi}) = \log(\epsilon^{2/5}\bar{\xi}) + \left[ y_+ + \frac{1}{2} \log(2\kappa) - \frac{1}{2} \log(1 - e^{-2\kappa}) \right] + \hat{y}(\bar{\xi}), \quad (\text{B.8})$$

$$z(\bar{\xi}) = \frac{1}{2} \log(\epsilon^{2/5}\bar{\xi}) + \left[ y_+ + \frac{1}{2} \log(2\kappa) - \frac{1}{2} \log(1 - e^{-4\kappa}) \right] + \hat{z}(\bar{\xi}). \quad (\text{B.9})$$

Note that the equation governing  $y$  is not singularly perturbed, so the terms that we denote by  $\hat{y}$  in (B.8) are small in the outer limit of the inner scaling compared to the leading order, and they do not affect the asymptotic matching. We can therefore discard these terms in the inner-region analysis for matched asymptotic expansions.

We write the governing equation (3.7) in inner variables. We retain terms up to leading order in  $\epsilon$  and obtain

$$2\epsilon^{1/5} \left[ -\frac{1}{2\bar{\xi}^2} + \frac{d^2 \hat{z}(\bar{\xi})}{d\bar{\xi}^2} \right] = -\epsilon^{1/5} \bar{\xi}^{-1/2} \beta^2 e^{-\hat{z}(\bar{\xi})} + \epsilon^{1/5} \bar{\xi}^{-1/2} \beta^2 e^{\hat{z}(\bar{\xi})}. \quad (\text{B.10})$$

We express  $\hat{z}$  in terms of the local series

$$\hat{z}(\xi) \sim \sum_{j=1}^{\infty} \frac{a_j}{\xi^{j/2}}, \quad \text{as } z \rightarrow 0, \quad (\text{B.11})$$

where the choice of  $j/2$  in the power is necessary to completely characterize the asymptotic series. We now expand the exponentials in equation (B.10) and use the resulting relationship to determine successive values of  $a_j$ . Using this relationship, we find that only every fifth term in the series beginning from  $j = 4$  (i.e.,  $a_{5j-1}$  for  $j \geq 1$ ) is nonzero. This is consistent with the local behavior of  $\chi$  in equation (B.6). Matching the inner expansion (B.11) with the outer ansatz (B.7) requires that

$$\frac{\Lambda}{\sqrt{\beta}} = \lim_{j \rightarrow \infty} \frac{a_{5j-1} (4/5)^{2j-1/10}}{\Gamma(2j-1/10)}. \quad (\text{B.12})$$

Values for  $a_j$  can be computed numerically by substituting the series expression (B.11) into the governing equation (B.10) and solving a recurrence relation for  $a_j$  in terms of the previous series coefficients. By computing  $a_j$  for sufficiently large values of  $j$  and substituting these values into (B.12), we solve the resulting expression for  $\Lambda$ . We find that  $\Lambda \approx -0.3500\sqrt{\beta}$  for both  $\xi_1$  and  $\xi_2$ . Calculating the value of  $\Lambda$  associated with  $\xi_3$  and  $\xi_4$  leads to a slightly different inner equation in place of (B.10), although the matching equation (B.12) is identical. In this case, we find that  $\Lambda \approx 0.3500\sqrt{\beta}$ .

### Appendix C. Stokes Smoothing.

Now that we have obtained late-order terms, we truncate the series after  $N$  terms to give

$$y(\xi) = \sum_{j=0}^{N-1} \epsilon^j y_j(\xi) + S_N(\xi), \quad z(\xi) = \sum_{j=0}^{N-1} \epsilon^j z_j(\xi) + R_N(\xi). \quad (\text{C.1})$$

To apply the exponential asymptotic technique of [18], we need to optimally truncate the series

(C.1). In the  $\epsilon \rightarrow 0$  limit, we need a large number of terms for an optimal truncation. Following [13], we determine the optimal truncation by finding the point at which consecutive terms in the series are equal in size. That is,

$$\left| \frac{\epsilon^{N+1} z_{N+1}(\xi)}{\epsilon^N z_N(\xi)} \right| \sim 1 \quad \text{as} \quad \epsilon \rightarrow 0. \quad (\text{C.2})$$

Using the general form of the ansatz (3.16), we obtain  $N \sim |\chi|/2\sqrt{\epsilon}$ . Consequently, we set the optimal truncation point to be

$$N = \frac{|\chi|}{2\sqrt{\epsilon}} + \omega, \quad (\text{C.3})$$

where we choose  $\omega \in [0, 1)$  to ensure that  $N$  is an integer.

We now apply the truncated series expression (C.1) to (3.1) and (3.2). Using the relation (3.11), we obtain as  $\epsilon \rightarrow 0$  that

$$\lambda S_N''(\xi) \sim R_N(\xi - 1)e^{-\frac{1}{2}[y_0(\xi) - y_0(\xi-1)]} + R_N(\xi)e^{-\frac{1}{2}[y_0(\xi+1) - y_0(\xi)]} + \dots, \quad (\text{C.4})$$

$$\epsilon \lambda R_N''(\xi) + 2e^{-\frac{1}{2}[y_0(\xi+1) - y_0(\xi)]} R_N(\xi) \sim -\lambda \epsilon^N z_{N-1}''(\xi) + \dots, \quad (\text{C.5})$$

where the omitted terms are smaller in magnitude than those that we retained in the equation by a factor of  $\epsilon$  or more in the limit that  $\epsilon \rightarrow 0$ . Throughout the remainder of this appendix, we will consider asymptotic behavior in the  $\epsilon \rightarrow 0$  asymptotic limit.

Applying the expression (3.19) for the singulant and the late-order term ansatz (noting again that  $N \rightarrow \infty$  as  $\epsilon \rightarrow 0$ ), we obtain

$$\epsilon \lambda R_N''(\xi) - \lambda \chi'(\xi)^2 R_N(\xi) \sim -\frac{\lambda \epsilon^N \chi'(\xi)^2 Z(\xi) \Gamma(2N - 1/10)}{\chi(\xi)^{2N-1/10}}. \quad (\text{C.6})$$

Away from the Stokes curve, the right-hand side of (C.6) is small compared to the terms on the left-hand side. Consequently, we find the behavior that switches on across the Stokes curve by considering the homogeneous solution to equation (C.6). We then use WKB analysis to determine that away from the Stokes curve,  $R_N \sim CZ e^{-\chi/\sqrt{\epsilon}}$  as  $\epsilon \rightarrow 0$ , where  $C$  is an arbitrary constant. In fact, because we have specified that oscillations cannot extend ahead of the traveling wave front, we know that  $C = 0$  to the left of the Stokes curve.

To determine the behavior near the Stokes curve, we write

$$R_N \sim A(\xi) Z(\xi, t) e^{-\chi(\xi, t)/\sqrt{\epsilon}} \quad \text{as} \quad \epsilon \rightarrow 0, \quad (\text{C.7})$$

where  $A(\xi)$  is a Stokes switching parameter that varies rapidly in the neighborhood of the Stokes curve. We henceforth omit the arguments for  $A$ ,  $Z$ , and  $\chi$ , as they are always identical to each

other. We find that (C.6) becomes

$$\epsilon \left[ \frac{AZ(\chi')^2}{\epsilon} - \frac{2A'Z\chi'}{\sqrt{\epsilon}} - \frac{2AZ'\chi'}{\sqrt{\epsilon}} - \frac{AZ\chi''}{\sqrt{\epsilon}} \right] e^{-\chi/\sqrt{\epsilon}} - (\chi')^2 AZ e^{-\chi/\sqrt{\epsilon}} \sim -\frac{\epsilon^N (\chi')^2 Z \Gamma(2N-1/10)}{\chi^{2N-1/10}}. \quad (\text{C.8})$$

Using (3.19) and (A.6), equation (C.8) reduces to

$$-2A'\chi' e^{-\chi/\sqrt{\epsilon}} \sim -\frac{\epsilon^{N-1/2} (\chi')^2 \Gamma(2N-1/10)}{\chi^{2N-1/10}} \quad \text{as} \quad \epsilon \rightarrow 0. \quad (\text{C.9})$$

We now write (C.9) in terms of  $\chi$  as an independent variable. Noting that  $A'(\xi) = \chi'(\xi) \frac{dA}{d\chi}$  and rearranging, we obtain

$$\frac{dA}{d\chi} \sim \frac{\epsilon^{N-1/2} \Gamma(2N-1/10)}{2\chi^{2N-1/10}} e^{\chi/\sqrt{\epsilon}}. \quad (\text{C.10})$$

We define polar coordinates and note that variation in  $\theta$  is much more rapid than variation in  $r$  near the Stokes curve. We thus see that

$$\chi = r e^{i\theta}, \quad \frac{d}{d\chi} = -\frac{i e^{-i\theta}}{r} \frac{d}{d\theta}. \quad (\text{C.11})$$

The optimal truncation in equation (C.3) then gives

$$\frac{dA}{d\theta} \sim i r e^{i\theta} \frac{\epsilon^{r/2\sqrt{\epsilon} + \omega - 1/2} \Gamma(r/\sqrt{\epsilon} + 2\omega - 1/10)}{2(r e^{i\theta})^{r/\sqrt{\epsilon} + 2\omega - 1/10}} e^{r e^{i\theta}/\sqrt{\epsilon}}. \quad (\text{C.12})$$

We now use an asymptotic expansion of the gamma function [1, 2] and expand equation (C.12) and simplify to obtain

$$\frac{dA}{d\theta} \sim i \sqrt{\frac{\pi}{2}} \epsilon^{-1/4 + 1/20} r^{1/2} \exp\left(\frac{r}{\sqrt{\epsilon}}(e^{i\theta} - 1) - \frac{i\theta r}{\sqrt{\epsilon}} + i\theta(1 + 1/10 + 2\omega)\right). \quad (\text{C.13})$$

The right-hand side of equation (C.13) is exponentially small in  $\epsilon$ , except in the neighborhood of  $\theta = 0$ . We therefore define an inner region  $\theta = \epsilon^{1/4} \bar{\theta}$  and thereby find that

$$\frac{dA}{d\theta} \sim i \sqrt{\frac{\pi}{2}} \epsilon^{1/20} r^{1/2} e^{-r\bar{\theta}^2/2}. \quad (\text{C.14})$$

Consequently, by integration, we see that the behavior as the Stokes curve is crossed is

$$A \sim i \sqrt{\frac{\pi}{2}} \epsilon^{1/20} r^{1/2} \int_{-\infty}^{\bar{\theta}} e^{-rs^2/2} ds \quad \text{as} \quad \epsilon \rightarrow 0. \quad (\text{C.15})$$

Therefore, as the Stokes curve is crossed from  $\bar{\theta} < 0$  to  $\bar{\theta} > 0$ , we find that

$$[A]_{-}^{+} \sim \pi i \epsilon^{1/20} \quad \text{as} \quad \epsilon \rightarrow 0 \quad (\text{C.16})$$

and hence that the combined exponentially-small contribution is given in the  $\epsilon \rightarrow 0$  limit by

$$[R_N]_{\pm}^{\pm} \sim \pi i \epsilon^{1/20} Z e^{-\chi/\sqrt{\epsilon}} + \text{c.c.}, \quad (\text{C.17})$$

where we include the complex-conjugate contribution. Because  $R_N(\xi)$  must be 0 ahead of the solitary wave (i.e., when  $\text{Im}(\chi) < 0$ ), we find that behind the wave front, the exponentially-small contribution is given in  $\epsilon \rightarrow 0$  limit by

$$R_N \sim \frac{\pi \Lambda i \epsilon^{1/20}}{\sqrt{\chi'(\xi)}} e^{-\chi(\xi)/\sqrt{\epsilon}} + \text{c.c.}. \quad (\text{C.18})$$

From equation (C.4), we see that the corresponding form of  $S_N(\xi)$  is given in the limit that  $\epsilon \rightarrow 0$  by

$$S_N \sim -\frac{\epsilon}{2} \left[ \frac{\pi \Lambda i \epsilon^{1/20}}{\sqrt{\chi'(\xi-1)}} e^{-\chi(\xi-1)/\sqrt{\epsilon}} + \frac{\pi \Lambda i \epsilon^{1/20}}{\sqrt{\chi'(\xi)}} e^{-\chi(\xi)/\sqrt{\epsilon}} \right] + \text{c.c.}. \quad (\text{C.19})$$

#### REFERENCES

- [1] Digital Library of Mathematical Functions. *National Institute of Standards and Technology*, 2015. Available at <http://dlmf.nist.gov/>; release 1.0.10 (2015-08-07).
- [2] M. Abramowitz and I. Stegun. *Handbook of Mathematical Functions with Formulas, Graphs, and Mathematical Tables*. Dover Publications, New York, 1972.
- [3] K. Ahnert and A. Pikovsky. Compactons and chaos in strongly nonlinear lattices. *Phys. Rev. E*, 79(2):026209, 2009.
- [4] T. R. Akylas and R. H. J. Grimshaw. Solitary internal waves with oscillatory tails. *J. Fluid Mech.*, 242:279–298, 1992.
- [5] J. M. Arnold. Complex Toda lattice and its application to the theory of interacting optical solitons. *J. Opt. Soc. Amer. A*, 15(5):1450–1458, 1998.
- [6] M. V. Berry. Stokes phenomenon; smoothing a Victorian discontinuity. *Pub. Math. de L’IHÉS*, 68:211–221, 1988.
- [7] M. V. Berry. Uniform asymptotic smoothing of Stokes’s discontinuities. *Proc. Roy. Soc. Lond. A*, 422(1862):7–21, 1989.
- [8] M. V. Berry. Asymptotics, superasymptotics, hyperasymptotics. In H. Segur, S. Tanveer, and H. Levine, editors, *Asymptotics Beyond All Orders*, pages 1–14. Plenum, Amsterdam, 1991.
- [9] M. V. Berry and C. J. Howls. Hyperasymptotics. *Proc. Roy. Soc. Lond. A*, 430(1880):653–668, 1990.
- [10] L. Bonanomi, G. Theocharis, and C. Daraio. Wave propagation in granular chains with local resonances. *Phys. Rev. E*, 91:033208, 2015.
- [11] J. P. Boyd. A numerical calculation of a weakly non-local solitary wave: the  $\phi^4$  breather. *Nonlinearity*, 3(1):177–195, 1990.
- [12] J. P. Boyd. *Weakly Nonlocal Solitary Waves and Beyond-All-Orders Asymptotics: Generalized Solitons and Hyperasymptotic Perturbation Theory*, volume 442 of *Mathematics and Its Applications*. Kluwer, Amsterdam, 1998.
- [13] J. P. Boyd. The devil’s invention: Asymptotic, superasymptotic and hyperasymptotic series. *Acta Appl. Math.*, 56(1):1–98, 1999.
- [14] J. P. Boyd. Hyperasymptotics and the linear boundary layer problem: Why asymptotic series diverge. *SIAM Rev.*, 47(3):553–575, 2005.
- [15] D. C. Calvo and T. R. Akylas. On the formation of bound states by interacting nonlocal solitary waves. *Physica D*, 101(3):270–288, 1997.
- [16] G. Casati and J. Ford. Stochastic transition in the unequal-mass Toda lattice. *Phys. Rev. A*, 12(4):1702–

- 1709, 1975.
- [17] G. A. Cassatella Contra and D. Levi. Discrete multiscale analysis: a biatomic lattice system. *J. Nonlinear Math. Phys.*, 17(03):357–377, 2010.
  - [18] S. J. Chapman, J. R. King, J. R. Ockendon, and K. L. Adams. Exponential asymptotics and Stokes lines in nonlinear ordinary differential equations. *Proc. Roy. Soc. Lond. A*, 454(1978):2733–2755, 1998.
  - [19] G. Darboux. Sur l’approximation des fonctions de très-grands nombres et sur une classe étendue de développements en série. *J de Math*, pages 377–416, 1878.
  - [20] P. C. Dash and K. Patnaik. Nonlinear wave in a diatomic Toda lattice. *Phys. Rev. A*, 23(2):959–969, 1981.
  - [21] P. C. Dash and K. Patnaik. Solitons in nonlinear diatomic lattices. *Prog. Theor. Phys.*, 65(5):1526–1541, 1981.
  - [22] M. Desroches, J. Guckenheimer, B. Krauskopf, C. Kuehn, H. M. Osinga, and M. Wechselberger. Mixed-mode oscillations with multiple time scales. *SIAM Review*, 54(2):211–288, 2012.
  - [23] S. Diederich. Dynamic form factors of the diatomic Toda lattice. *J. Phys. C*, 18(18):3415–3425, 1985.
  - [24] R. B. Dingle. *Asymptotic Expansions: Their Derivation and Interpretation*. Academic Press, New York, 1973.
  - [25] J. English and R. Pego. On the solitary wave pulse in a chain of beads. *Proc. Amer. Math. Soc.*, 133(6):1763–1768, 2005.
  - [26] L. Faddeev and L. Takhtajan. *Hamiltonian Methods in the Theory of Solitons*. Springer Science & Business Media, 2007.
  - [27] E. Fermi, J. Pasta, and S. Ulam. Studies of Nonlinear Problems. I. (*Los Alamos National Laboratory, Los Alamos, N. M.*), Tech. Rep.:LA–1940, 1955.
  - [28] S. Flach. Nonlinear lattice waves in random potentials. In C. Besse and J. C. Garreau, editors, *Nonlinear Optical and Atomic Systems*, volume 2146 of *Lecture Notes in Mathematics*, pages 1–48. Springer, 2015.
  - [29] G. Gantzounis, M. Serra-Garcia, K. Homma, J. M. Mendoza, and C. Daraio. Granular metamaterials for vibration mitigation. *J. Appl. Phys.*, 114:093514, 2013.
  - [30] R. Grimshaw. Exponential asymptotics and generalized solitary waves. In H. Steinrück, F. Pfeiffer, F. G. Rammerstorfer, J. Salençon, B. Schrefler, and P. Serafini, editors, *Asymptotic Methods in Fluid Mechanics: Survey and Recent Advances*, volume 523 of *CISM Courses and Lectures*, pages 71–120. Springer Vienna, 2011.
  - [31] R. Grimshaw and N. Joshi. Weakly nonlocal solitary waves in a singularly perturbed Korteweg-de Vries equation. *SIAM J. Appl. Math.*, 55(1):124–135, 1995.
  - [32] T. Hatano. Heat conduction in the diatomic Toda lattice revisited. *Phys. Rev. E*, 59(1):R1–R4, 1999.
  - [33] R. Hirota and K. Suzuki. Theoretical and experimental studies of lattice solitons in nonlinear lumped networks. *Proc. IEEE*, 61(10):1483–1491, 1973.
  - [34] M. Hörnquist and R. Riklund. Solitary wave propagation in periodic and aperiodic diatomic Toda lattices. *J. Phys. Soc. Jpn.*, 65(9):2872–2879, 1996.
  - [35] K. R. Jayaprakash, Y. Starosvetsky, and A. F. Vakakis. New family of solitary waves in granular dimer chains with no precompression. *Phys. Rev. E*, 83(3):036606, 2011.
  - [36] K. R. Jayaprakash, Y. Starosvetsky, A. F. Vakakis, and O. V. Gendelman. Nonlinear resonances leading to strong pulse attenuation in granular dimer chains. *J. Nonlinear Sci.*, 23(3):363–392, 2013.
  - [37] P. G. Kevrekidis, A. Stefanov, and H. Xu. Traveling waves for the mass in mass model of granular chains. *Lett. Math. Phys.*, pages 1–22, 2016.
  - [38] E. Kim, F. Li, C. Chong, G. Theocharis, J. Yang, and P. G. Kevrekidis. Highly nonlinear wave propagation in elastic woodpile periodic structures. *Phys. Rev. Lett.*, 114(11):118002, 2015.
  - [39] E. Kim and J. Yang. Wave propagation in single column woodpile phononic crystals: Formation of tunable band gaps. *J. Mech. Phys. Solids*, 71:33–45, 2014.
  - [40] Y. S. Kivshar and N. Flytzanis. Gap solitons in diatomic lattices. *Phys. Rev. A*, 46(12):7972–7978, 1992.
  - [41] T. Kofane, B. Michaux, and M. Remoissenet. Theoretical and experimental studies of diatomic lattice solitons using an electrical transmission line. *J. Phys. C*, 21(8):1395–1412, 1988.
  - [42] T. Kuusela, J. Hietarinta, and B. A. Malomed. Numerical study of solitons in the damped AC-driven Toda lattice. *J. Phys. A*, 26(1):L21–L26, 1993.

- [43] T. V. Laptyeva, M. V. Ivanchenko, and S. Flach. Nonlinear lattice waves in heterogeneous media. *J. Phys. A: Math. Theor.*, 47:493001, 2014.
- [44] L. Liu, G. James, P. Kevrekidis, and A. Vainchtein. Nonlinear waves in a strongly nonlinear resonant granular chain. *arXiv preprint arXiv:1506.02827*, 2015.
- [45] C. J. Lustrì, S. W. McCue, and B. J. Binder. Free surface flow past topography: A beyond-all-orders approach. *Euro. J. Appl. Math.*, 23(4):441–467, 2012.
- [46] Alejandro J. Martínez, P. G. Kevrekidis, and Mason A. Porter. Superdiffusive transport and energy localization in disordered granular crystals. *Phys. Rev. E*, 93:022902, 2016.
- [47] F. Mokross and H. Büttner. Comments on the diatomic Toda lattice. *Phys. Rev. A*, 24(5):2826–2828, 1981.
- [48] F. Mokross and H. Büttner. Thermal conductivity in the diatomic Toda lattice. *J. Phys. C*, 16(23):4539–4546, 1983.
- [49] M. Moleron, A. Leonard, and C. Daraio. Solitary waves in a chain of repelling magnets. *J. App. Phys.*, 115:184901, 2014.
- [50] V. F. Nesterenko. *Dynamics of Heterogeneous Materials*. Springer-Verlag, 2001.
- [51] Y. Okada, S. Watanabe, and H. Tanaca. Solitary wave in periodic nonlinear lattice. *J. Phys. Soc. Jpn.*, 59(8):2647–2658, 1990.
- [52] A. B. Olde Daalhuis, S. J. Chapman, J. R. King, J. R. Ockendon, and R. H. Tew. Stokes phenomenon and matched asymptotic expansions. *SIAM J. App. Math.*, 55(6):1469–1483, 1995.
- [53] F. W. J. Olver, D. W. Lozier, R. F. Boisvert, and C. W. Clark. *NIST Handbook of Mathematical Functions*. Cambridge University Press, New York, NY, 2010.
- [54] St. Pnevmatikos, N. Flytzanis, and M. Remoissenet. Soliton dynamics of nonlinear diatomic lattices. *Phys. Rev. B*, 33:2308–2321, 1986.
- [55] M. A. Porter, C. Daraio, I. Szelengowicz, E. B. Herbold, and P. G. Kevrekidis. Highly nonlinear solitary waves in heterogeneous periodic granular media. *Physica D*, 238(6):666–676, 2009.
- [56] M. A. Porter, P.G. Kevrekidis, and C. Daraio. Granular crystals: Nonlinear dynamics meets materials engineering. *Phys. Today*, 68(11):44–50, 2015.
- [57] M. A. Porter, N. J. Zabusky, B. Hu, and D. K. Campbell. Fermi, Pasta, Ulam and the birth of experimental mathematics. *Am. Sci.*, 97(3):214–221, 2009.
- [58] M. J. D. Powell. A FORTRAN subroutine for solving systems of nonlinear algebraic equations. Technical report, Atomic Energy Research Establishment, Harwell (England), 1968.
- [59] W.-X. Qin. Wave propagation in diatomic lattices. *SIAM J. Math. Anal.*, 47(1):477–497, 2015.
- [60] A. V. Savin and O. V. Gendelman. Heat conduction in one-dimensional lattices with on-site potential. *Phys. Rev. E*, 67(4):041205, 2003.
- [61] H. Segur and M. D. Kruskal. Nonexistence of small-amplitude breather solutions in  $\phi^4$  theory. *Phys. Rev. Lett.*, 58(8):747–750, 1987.
- [62] S. Sen, J. Hong, J. Bang, E. Avalos, and R. Doney. Solitary waves in the granular chain. *Phys. Rep.*, 462(2):21–66, 2008.
- [63] S. Sen and M. Manciu. Discrete Hertzian chains and solitons. *Physica A*, 268(3):644–649, 1999.
- [64] G. G. Stokes. On the discontinuity of arbitrary constants which appear in divergent developments. *Trans. Cam. Phil. Soc.*, 10:106–128, 1864.
- [65] Y. Tabata. Stable solitary wave in diatomic Toda lattice. *J. Phys. Soc. Jpn.*, 65(12):3689–3691, 1996.
- [66] M. Toda. Wave propagation in anharmonic lattices. *J. Phys. Soc. Jpn.*, 23(3):501–506, 1967.
- [67] M. Toda. *Theory of Nonlinear Lattices*, volume 20. Springer Science & Business Media, 2012.
- [68] P. H. Trinh and S. J. Chapman. New gravity-capillary waves at low speeds. Part 2. Nonlinear geometries. *J. Fluid Mech.*, 724:392–424, 2013.
- [69] P. K. A. Wai, H. H. Chen, and Y. C. Lee. Radiations by “solitons” the zero group-dispersion wavelength of single-mode optical fibers. *Phys. Rev. A*, 41(1):426–439, 1990.
- [70] H. Xu, P. G. Kevrekidis, and A. Stefanov. Traveling waves and their tails in locally resonant granular systems. *J. Phys. A*, 48(19):195204, 2015.
- [71] N. Yajima and J. Satsuma. Soliton solutions in a diatomic lattice system. *Prog. Theor. Phys.*, 62(2):370–378, 1979.
- [72] Y. Zhang and H. Zhao. Heat conduction in a one-dimensional aperiodic system. *Phys. Rev. E*, 66(2):026106,

2002.